

Article

A Multi-wavelength View of OJ 287 Activity in 2015-2017: Implications of Spectral Changes on Central-engine Models and MeV-GeV Emission Mechanism

Pankaj Kushwaha*  0000-0001-6890-2236

Department of Astronomy (IAG-USP), University of Sao Paulo, Sao Paulo 05508-090, Brazil
Aryabhata Research Institute of Observational Sciences (ARIES), Nainital 263002, India

Version February 7, 2020 submitted to *Galaxies*

Abstract: A diverse range of observational results and peculiar properties across the domains of observation have made OJ 287 one of the best-explored BL Lac objects on the issues of relativistic jets and accretion physics as well as the strong theory of gravity. We here present a brief compilation of observational results from the literature and inferences/insights from the extensive studies but focus on the interpretation of its ~ 12 -yr quasi-periodic optical outbursts (QPOOs) and high energy emission mechanisms. The QPOOs in one model are attributed to the disk-impact related to dynamics of the binary SMBHs while alternative models attribute it to the geometrical effect related to the precession of a single jet or double jets. We discuss implications of the new spectral features reported during the 2015–2017 multi-wavelength high activity of the source – a break in the NIR-optical spectrum and hardening of the MeV-GeV emission accompanied by a shift in the location of its peak, in the context of the two. The reported NIR-optical break nicely fits the description of a standard accretion disk emission from an SMBH of mass $\sim 10^{10} M_{\odot}$ while the time of its first appearance in end-May 2013 (MJD 56439) is in close coincidence with the time of impact predicted by the disk-impact binary SMBH model. This spectral and temporal coincidence with the model parameters of the disk-impact binary SMBH model provides independent evidence in favor of the model over the geometrical models which argue a total central-engine mass in the range of $10^{7-9} M_{\odot}$. On the other hand, the MeV-GeV spectral change is naturally reproduced by the inverse Compton scattering of photons from the broad-line region and is consistent with the detection of broad emission lines during the previous cycles of quasi-periodic outbursts. Combining this with previous SED studies suggests that in OJ 287, MeV-GeV emission results from external Comptonization.

Keywords: BL Lac objects: individual: OJ 287 – galaxies: active – galaxies: jets – radiation mechanisms: non-thermal– gamma-rays: galaxies

1. Introduction

Non-thermal emission is ubiquitous with jets hosted by compact astrophysical objects being one of the most prominent emitters. One of the most powerful and persistent jets are those found in active galactic nuclei (AGNs) designated radio-loud, characterized by a large scale, highly collimated, relativistic jets of plasma. In particular, the subclass called blazar – AGNs with bipolar relativistic jets of plasma aligned to our line of sight has its entire emission almost fully dominated by the jet emission. They have been found to emit across the entire electromagnetic (EM) spectrum, from radio to GeV-TeV energies [~ 17 – 20 orders of magnitude; e.g. 1], variable on all timescales from orders of a few 10s of

minutes and even less to decades¹ [~ 6 – 7 orders of magnitude; e.g. 2]. Their radio and optical emission is highly polarized and have been observed to vary often with the source flux, all the way from 0 to $> 50\%$. Imaging in radio, infra-red (IR), optical, and X-ray, on the other hand, show an extremely well collimated jet extending up to Mpc scales [~ 9 – 13 orders of magnitude; e.g. 3,4] with frequent sighting of superluminal features in high-resolution imaging of the core. Taken together with the observational and theoretical understanding of other astrophysical objects combined with their high and rarely repeating observational behavior indicates that they are the site of complex, multi-level, multi-scale physics and thus, are normally called extreme sources among non-catastrophic events.

Though studies in different energy bands finally culminated into a unified scheme for radio-loud AGNs [5], it also revealed that AGNs need well-coordinated multi-wavelength (MW) observations to go beyond the limits associated with individual bands. The launch of the gamma-ray survey observatory *Fermi*-LAT (Large Area Telescope) with an unprecedented MeV-GeV sensitivity [6] has revolutionized studies of γ -ray emitting sources, especially blazars. The *Fermi* AGN monitoring program² supported by a host of observatories across the globe, working in different energy bands and supplementing and coordinating *Fermi* observations currently serves as the best archive of (relatively) unbiased data. The *Fermi*-LAT survey catalog, as was expected, revealed blazars (and AGNs) as the largest source population, making $>60\%$ of the detected sources [4FGL; 7]. This allowed a detailed spectral, temporal, polarization, and imaging characterization of blazars, as well as exploration of correlations between them, thereby greatly enhancing our understanding of these sources and physical conditions within the relativistic jets.

Spectral and temporal studies, in particular, high energy (HE) emission mechanisms and search for (quasi) periodic modulation has been one of the focus of intensive research, in addition to characterization based on these. Temporal studies of flux variability have firmly established it to be stochastic with statistical properties [2,8,9] broadly similar to those exhibited by other-accretion powered sources [10]. Though a few cases of firm quasi-periodic signals have been observed, significance of most of the detected signal is still marginal [e.g. 11, and references therein]. Broadband spectral studies, on the other hand, revealed a characteristic broad double-humped spectral energy distribution (SED). This feature culminated in a new classification scheme for blazars based on the frequency (ν_p) at which the low-energy component peaks [1,12]. Thus, sources with $\nu_p < 10^{14}$ Hz, $10^{14} < \nu_p < 10^{15}$, and $\nu_p > 10^{15}$ are respectively called as low-synchrotron peaked (LSP), intermediate-synchrotron peaked (ISP), and high-synchrotron peaked (HSP) blazars. So far only BL Lacs (BLLs) subclass of blazars have been found to exhibit the three spectral classes, referred to respectively as low-frequency-peaked BL Lacs (LBLs), intermediate-energy-peaked BL Lacs (IBLs), and high-frequency-peaked BLLs (HBLs) [12] whereas flat spectrum radio quasars (FSRQs) so far are exclusively LSP sources.

The low-energy hump of the blazars SED extends from radio to ultraviolet(UV)/X-ray energies, attaining a maximum in between NIR to soft-X-rays and is widely regarded as the synchrotron emission from a relativistic non-thermal electron in the jet. The high-energy hump spans X-rays to GeV–TeV energies, peaking in MeV-GeV energies, but its origin remains uncertain. The uncertainty is a direct reflection of lack of constraint on the matter content of the jet plasma, whether mainly electrons (leptonic) and/or hadrons (protons primarily) and particle acceleration. Within the limit of current observational constraints, both the models have been successful in explaining observed broadband SEDs [e.g. 13–16] though the exact cause and the level of contribution/dominance remains a matter of debate. In the leptonic scenario, entire broadband emission is attributed to the primary electrons, via synchrotron at radio to UV/X-ray energies and via inverse Compton (IC) scattering from X-ray up to TeVs [e.g. 16–18]. Until recently, this has been the most favored interpretation of blazar emission

¹ currently feasible with observing facilities and available data

² Multi-wavelength support program – <https://fermi.gsfc.nasa.gov/ssc/observations/multi/programs.html>

due to the photon rich environment offered by the AGNs constituents for IC scattering e.g. accretion disk (AD) close to the source, broad-line region (BLR) with extension up to sub-parsec scales, infra-red torus on parsec (pc) scales, and the omnipresent cosmic microwave background (CMB), in addition to the synchrotron photons. The respective IC scattered radiation, in blazar community, are referred to as EC-AD [19], EC-BLR [20], EC-IR [20], EC-CMB, and synchrotron self-Compton [SSC; 21] where EC stands for External Comptonization – IC scattering of photon field external to the jet. Depending on the location of the emission region, one or many of the photon fields can contribute and/or dominate the scattering process. In general, FSRQs requires EC to explain their γ -ray emission while SSC is sufficient for most of the BLLs (IBLs and HBLs). Given the current understanding of emission lines strength in the sub-classes of blazar [22, and references therein], it seems that to a broad basic level, the traditional sub-classification of blazars based on rest-frame equivalent width (EW) of optical emission lines into BL Lacertae objects (BLLs, $EW < 5 \text{ \AA}$) and flat spectrum radio quasars (FSRQs, $EW > 5 \text{ \AA}$) nicely integrate into the interpretation that in BLLs the high-energy hump is primarily powered by SSC while its by EC in FSRQs.

The hadronic scenario attributes the HE hump to proton synchrotron (purely electromagnetic process) and/or cascade initiated as a result of interaction of ultra-relativistic protons ($\geq EeV$) with photons and/or protons³ [e.g. 14]. The recent detection of a ~ 290 -TeV neutrino (IceCube-170922A) by the *IceCube* observatory in the direction of blazar TXS 0506+056 [23,24], spatially and temporally coincident with its flaring MW activity provided the first clear evidence in favor of hadronic emission. Further investigation of data revealed neutrinos detection in the same direction during a quiescent state of the source [23]. Though interpretations of these neutrinos are still under debate [25, and references therein], modeling of SEDs corresponding to the neutrino episodes suggests an overall sub-dominant hadronic contribution [26].

Majority of the blazars MW activities have been observed to be simultaneous within the observational cadence. With radio to optical emission being synchrotron, the standard leptonic scenario provides the simplest, natural and logical explanation to such highly correlated variability though more complex physical processes may be involved and thus, more involved interpretations can be offered [e.g. 27]. For BLLs, in the standard leptonic picture, an SSC interpretation has been generally favored in the literature for their HE hump due to a weak or absent BLR field. However, increasing number of studies suggest that this may not be true for LBLs and instead argue EC-IR for the MeV–GeV emission [22,28,29]. For example, in the case of 2009 flare of LBL OJ 287, Kushwaha *et al.* [28] have shown the in-feasibility of SSC in explaining MeV–GeV emission through a systematic modeling of SEDs within the observational constraints while for LBL AO 0235+164, Ackermann *et al.* [22] have argued the EC interpretation based on energetics and the luminosity of the detected emission lines. The inability of SSC to reproduce the X-ray and γ -ray emission in the case of OJ 287 was already apparent from the work of Seta *et al.* [30], with the only exception being the lack of a contemporaneous MeV–GeV spectrum. The EC-IR interpretation of MeV–GeV gamma-ray emission in these two is consistent with inferences drawn from the study of broadband SEDs of a sample of LBLs with good quality γ -ray spectra from *Fermi*-LAT [29]. A similar (EC-IR) interpretation is favored for FSRQs from the lack of spectral cutoff at $\gtrsim 20 \text{ GeV}$, expected due to the $\gamma - \gamma$ interaction, in the spectra extracted from ~ 7.3 -yr of *Fermi*-LAT [31]. However, this interpretation has an important caveat in the case of FSRQs. FSRQs are believed to have a rich IR torus field and the expected spectral cutoff due to $\gamma - \gamma$ interaction for it will occur at very high energies (VHEs, $E > 100 \text{ GeVs}$). Thus, spectra extracted from data integrated over a long duration may contain moments when the emission has mainly happened at parsec scales (EC-IR) for which the mentioned cutoff will not lie in *Fermi*-LAT band and thus, may hide/suppress the cutoff feature.

³ being the biggest constituent, almost exclusively

In the present work, we focus on the blazar OJ 287 – a potential binary SMBH candidate system. In particular, we discuss the implications of the new spectral features observed during its 2015-2017 MW activity on the source central engine models discussed in the literature and high energy emission (MeV – GeV) mechanisms – one of the fundamental debate in the blazar community and focus of intensive studies. First, we present a brief historical account of the source general properties as gleaned from observations and models/interpretations offered, if any, for its unique features in the next section. In §3, we discuss the implications of the reported features in the context of the main theme of the work with summary in §4. We have assumed a Λ CDM cosmology with $\Omega_M = 0.286$, $\Omega_\Lambda = 0.714$, and a Hubble constant $H_0 = 69.6$ km/s/Mpc. With this, OJ 287 redshift of 0.306 corresponds to a luminosity distance of 1.6 Gpc and an angular diameter scale of 4.556 kpc/arcsec.

2. OJ 287

OJ 287, as it is called now, was first reported in the second section of the VRO (Vermilion River Observatory) survey at 610.5 MHz [VRO 20.08.01; 32] and its optical association was identified by Blake [33]. Spectroscopic attempts following its identification failed to reveal any emission and or absorption features [34,35] and was firmly established only later at $z = 0.306$ when it was in a low flux state [36,37]. However, photo-polarimetric studies in radio to optical bands, in general, found it to be similar to other radio sources with a star-like appearance in optical images, inverted radio spectrum, variable brightness, polarized and variable non-thermal continuum [34,35,38–41]. These findings and resemblance of its flux and polarization variations with the archetypal source BL Lacartae, it was classified as a BL Lac type object [34]. These observations also found it to be the most dynamic among all, with comparable variations over a broad range of wavelengths [radio and optical; 34]. As a result, OJ 287 became the key source to characterize and understand the BL Lac class [36]. Subsequently, many focused as well as coordinated multi-wavelength studies were carried out in both photometric and photopolarimetric modes [e.g. 35,39,41,42].

Initial concerted efforts revealed a tantalizing ~ 39.2 -minute periodic signal in the optical observation while historical data archive revealed data going back to 1890 with four clear high activity duration of several months [41]. OJ 287, however, became famous after the discovery of persistent quasi-periodic outbursts (QPOs) of ~ 12 -yr in the optical band by Sillanpaa *et al.* [43]. Various models have been proposed in the literature for this repeating modulation and can be broadly grouped into two classes: dynamical and geometrical. The dynamical models attribute the recurring outbursts to accretion dynamics in a supermassive binary black holes (SBBHs) system [43–45] while geometrical models attribute it to Doppler boosted jet emission resulting from the jet precession [e.g. 46–48, and references therein].

The very first model by Sillanpaa *et al.* [43] postulated OJ 287 as an SBBH system. The outbursts in the model were result of enhanced accretion to the primary as a result of perturbation caused by the secondary when transiting the periastron in an orbit coplanar with the primary's accretion disk. It was based on the similarity of flare profiles and its structure to that of an accreting system [49]. The model successfully passed its first observational test by correctly predicting the 1994 optical outburst [50]. However, the intensive monitoring of the 1994 outburst revealed double-peaked flares with rather sharp substructures within it compared what was expected from an accretion flow [51]. Further, Sillanpaa *et al.* [43] model failed to explain the twin nature of the outbursts. This led Lehto and Valtonen [44] to propose the twin outbursts to be due to the impact of the secondary SMBH on the accretion disk of the primary twice every orbit (see also Sundelius *et al.* [52]). It attributed the outbursts to hot bubble of gas, torn off from the disk as a result of the impact which when expands and become optically thin, emits strongly in optical-UV bands via thermal bremsstrahlung. The flare emission is thus completely unpolarized. Another model in the dynamical class is by Tanaka [53]. It is based on theoretical studies and numerical hydrodynamic/magneto-hydrodynamic simulations of nearly equal-mass binary SMBH systems going around each other in an orbit coplanar with their circumbinary disk. For OJ 287, it assumes a total mass of $\sim 10^9 M_\odot$. The QPOs occur due to leakage

of gas into this cavity once every orbit. Though the model generates double flares, it has not been investigated in detail vis-a-vis the vast amount of available observational data on OJ 287. Thus, though it remains a plausible interpretation, the details are still to be worked out and tested with the available data.

Several other models, mainly based on geometrical interpretations have been proposed in the literature with earliest ones based solely on the recurrent double-peaked optical outbursts [46,54] while subsequent ones considering other observed inputs of OJ 287 like radio measurements [55,56], optical polarization [57], morphological changes [47] and jet kinematic features on parsec scales [48,58]. Except for Valtaoja *et al.* [55] and Villforth *et al.* [57] models, the recurring outbursts in these models are attributed to the Doppler boosting caused by systematic changes in the jet orientation with respect to our line of sight as a result of precession. In the model of Katz [46], the gravitational torque of the secondary induces precession in the primary's accretion disk which in turn leads to jet precession and cause the first flare. It attributes the second outburst to the nodding motion. Villata *et al.* [54] model argue that both the SMBH have precessing relativistic jets. The interaction between jet plasma and the ambient medium leads to the bending of the jets and the double-peaked outbursts arise when the bent jets are aligned towards us as a result of precession. Valtaoja *et al.* [55] proposed a hybrid interpretation for the twin outbursts based on the radio variability where they found that the first optical outburst has no radio counterpart while the second shows simultaneous radio and optical flares. They attributed the first flare to the disk impact and the second to the jet, resulting from the propagation of impact disturbances to the primary's jet. Another double jet model is proposed by Shi *et al.* [56] by additionally considering variability in radio and "double minimum" in the optical data. They interpret the double-peaked flares to the synchrotron emission from the double helix jet which appears partially merged at radio, giving rise to a broad temporal profile in radio bands.

The most recent and detailed models in the series of geometrical interpretations are by Britzen *et al.* [47] and Qian [48]. Britzen *et al.* [47] found a ~ 22 -yr periodicity in the morphological features of the parsec-scale jet. Assuming no abrupt changes in these kinematic features, they interpreted both the recurrent outbursts in optical and radio bands to Doppler boosted jet emission as a result of precessing and jet rotation. They further argue that a binary system is not needed and even a precessing accretion disk can generate the jet precession. Qian [48], on the other hand, showed that the trajectories of superluminal radio knots seen at 15 GHz and 43 GHz can be explained in a binary SMBH scenario with both SMBHs having precessing jets. Using the correlation between OJ 287 high activity and ejection of superluminal knots, Qian [48] further showed that the QPOs can be explained by the motion of a few of these knots. A completely different interpretation for the recurrent outbursts is proposed by Villforth *et al.* [57] from the study of optical photopolarimetric properties from 2005 to 2009. They attributed the observed features to the 'magnetic breathing' of the disk causing accretion of magnetic field lines and claimed that there should be no more such outbursts in the future.

As stated above, OJ 287 is a very dynamic source and the diversity of peculiar features have made it the best-monitored BLL blazar over a wide range of scales in all the domains of observation e.g. spectral: [27,28,39,59,60]; temporal: [2,43,59,61–64], Imaging: [4,65]; polarization:[59,66–68] on the aspects of jet, accretion physics, and test of the general theory of relativity. Below we list different observational facets of the source from the literature in each of the domains and inferences from these. It should, however, be noted that for some of the domains there is no clear boundary due to the method of detection used in some of the energy bands (e.g. radio measurement are primarily imaging and thus observation at different epoch provide temporally-sequenced data, thereby mixing the two). Further, the list of literature cited/mentioned in the context of observational features is neither exhaustive nor complete, but rather a practical consideration. In addition to citing studies reporting new features/properties and/or performing extensive analysis, we have followed a simple guiding principle where only references with earliest and latest observations are mentioned if the reported features/properties are similar.

2.1. Spectral

The general broadband SEDs of the source is typical of LSP/LBL subclass of blazars with emission up to GeV energies [1,28]. Reported SEDs suggest the low-energy component peak at \lesssim NIR bands and \lesssim 100 MeV for the high-energy component [1,28,59]. So far no shift in the location of the peak of the low-energy component has been observed, though additional emission component, similar to an HBL SED [27] was recently seen during its first-ever reported VHE activity [69]. Studies in different energy bands at different flux states of the source, however, have reported a wide variety of spectral features.

At radio centimeter wavelengths, it shows a convex (positive curvature) spectra [33], typical of the synchrotron self-absorbed quasi-stellar sources. This changes to power-law spectra representing optically thin synchrotron emission at mm wavelengths [35,70]. At NIR-Optical-UV energies, reported spectra can be separated into two groups. The first group corresponds to the duration before mid-2013 (MJD < 56439) when data in these bands are smoothly connected, irrespective of the source flux state and occasionally show hints of smooth curvature at either or both ends [28,30,35,39,59,63,66,70–72]. This includes spectra measured during the epochs of outbursts claimed to have a thermal origin in the binary SMBH model of Lehto and Valtonen [44]. All these are consistent with synchrotron emission from a power-law particle distribution. From mid-2013 (May 2013, MJD 56439, fig. 1-c) till February 2016 (MJD \sim 57455; fig. 1-d), a spectral break was observed at the junction of the NIR-optical region [60]. After February 2016, it again returned to its typical pre mid-2013 spectral state.

In contrast, at X-ray energies, it has been observed with most of the major X-ray facilities and has exhibited drastic spectral variations compared to the other EM bands. The observed spectra cover all the possible spectral phases. In addition to its typical LBL spectra described by a power-law photon spectral index of $\Gamma \sim 1.5$ -1.7 [$f_\nu \sim \nu^{-\Gamma}$; 28,30,60,73,74], it has shown a flat [$\Gamma \sim 1$; 27,28,63,75], extremely soft $\Gamma > 2$ [27,69,73, and references therein] as well as mixture of these [27,74,76]. Interestingly, most of the extremely soft spectral state seems to have been around (within a few years) the period of optical outbursts claimed to be thermal bremsstrahlung emission [44,77]. The latest steep X-ray spectral state was seen during the VHE activity of the source in 2017 [69] which also corresponds to the highest-ever reported X-ray emission from OJ 287 [27, and references therein].

Spectral inferences at gamma-rays before *Fermi*-LAT have only been indirect. A probable detection was claimed in the *Compton Gamma-Ray Observatory* (CGRO) energy band on board the *EGRET* during a high optical state of the source in 1994 [75]. Though photon statistics prevented spectral analysis, it was argued to be in a “hard” state based on the number of detected GeV photons. In the *Fermi*-LAT era, on the contrary, it is one of the bright MeV-GeV sources detected in the first 3-month of its operation with spectrum being consistent with a power-law profile [1]. Till date, all the reported MeV-GeV spectra before its latest activity starting November 2015 show a power-law [28] profile and suggest SED peak at \lesssim 100 MeV. The November 2015 MW activity revealed a hardened MeV-GeV spectrum with a shift in the HE SED peak and yet to revert to its generic form as per the latest records [27,60,69]. It also registered its first VHE activity [69] in 2016, accompanied by a change in MeV-GeV spectral state which is consistent with the extrapolated VHE spectrum [27]. The VHE activity was a transient phase, lasted about six months with source HE spectrum being of an LBL+HBL source [27]. Following this, OJ 287 has been added to the TeV source catalog⁴. A snippet of different spectral states exhibited by OJ 287 is shown in Figure 1.

2.2. Temporal

OJ 287 has shown variability on all time scales (e.g. minutes-to-hours: [59,78], days: [28,59], months-to-years: [41,59,62], decades: [43,61]) across the entire electromagnetic spectrum [e.g. 27,28,

⁴ <http://tevcat.uchicago.edu/>

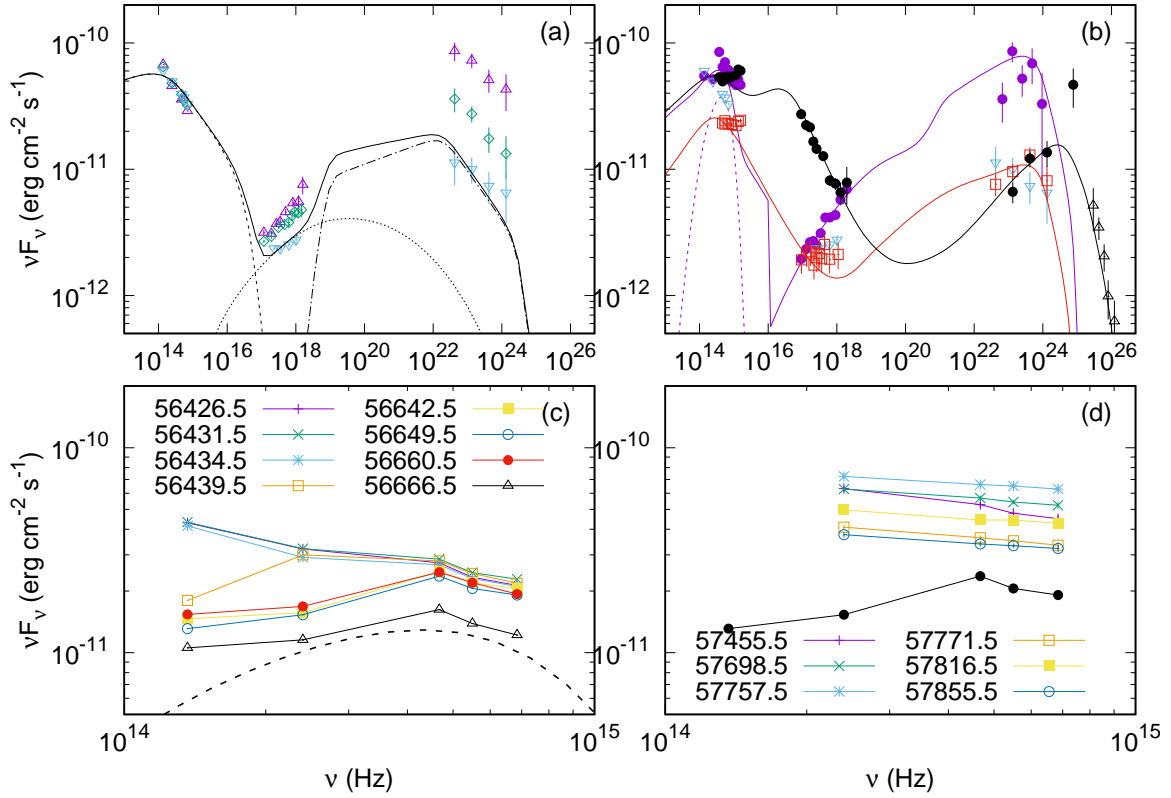


Figure 1. Broadband and optical SEDs showing the spectral phases exhibited by OJ 287 to date. (a) Typical broadband SEDs of OJ 287 from a 2009 observation [28] showing three different flux states: Flare (magenta, MJD: 55124-55131), moderate (green, MJD: 55131-55152) and quiescent (cyan, MJD: 55152-55184) in MW emission. The solid curve is the total emission with synchrotron, SSC and EC-IR component shown respectively in dashed, dotted, and dot-dashed curves [see 28, for modeling details]. (b) Broadband SEDs of the source in its new spectral phase during 2016-2017 with magenta (MJD: 57359-57363; [60]) showing a flare SED, black (MJD: 57786; [27]) showing a typical SED during the VHE phase and red (MJD: 57871; [27]) showing the quiescent SED state after the VHE activity with the lowest flux across EM spectrum. For reference/comparison, the quiescent SED (cyan) from panel (a) is also shown. The solid curves are the model produced spectrum [27,60, for details] while the dotted curve is the standard accretion-disk spectrum of a $\sim 10^{10} M_\odot$ SMBH. (c) NIR-optical spectrum highlighting the timing of the appearance of spectral break [60]. The dashed curve is the accretion-disk spectrum drawn again for clarity. (d) NIR-optical SEDs before (MJD 57455.5), during and after the VHE activity of OJ 287, showing return to the typical power-law NIR-optical spectrum. For comparison, one of the SED (black) from (c) is also shown.

[60,70]. On short time scales ($<$ months), it normally exhibits variation from NIR to MeV-GeV γ -ray energies which have been simultaneous within the observational cadence [e.g. 27,28,60]. An exception to this was the August 2016 – July 2017 (MJD: 57600 – 57950) period when simultaneous variation was seen only at optical to X-rays energies but statistically no variability at Fermi-LAT energies [27].

On long terms, MW variations, in general, are more pronounced at optical energies than X-rays but show no relation/pattern between the two [63]. In the Fourier domain, MW variations show flicker/colored-noise spectra on all timescales with γ -ray variation being different from the others. Statistical analyses of the radio to X-ray light curves show colored-noise power spectral densities (PSDs) for all and consistent with each other. Gamma-ray time series from LAT, on the other hand, shows both white and color noise PSD with the transition occurring on a timescale of 150-days [2]. Apart from stochastic variations, OJ 287 has also exhibited (quasi) periodic modulation and in fact, is the only blazar/AGN with the most numerous claims of QPOs of different duration in different energy

bands e.g. optical: ~ 40 minutes [41,79], 0-50 days [80], ~ 400 -days [81], ~ 11.65 years [43,47]; radio: ~ 16 minutes [82], 1.12 up 6-7 years [47, and references therein].

2.3. Imaging

At radio wavelengths, OJ 287 exhibits a one-sided jet with complex patterns on parsec [65,83] and kilo-parsec scales. Morphologically, it appears as an FR I source but energetically exhibits an FR II power. On Very Long Baseline Array (VLBA) resolution scales, it presents very complex dynamical patterns [65] with a core-jet structure [83,84], changes in jet position angle as well as overall morphology on parsec scales [65,67,84]. Tateyama and Kingham [84] study of kinematic features at 8 GHz has reported a clockwise change of $\sim 30^\circ$ in jet position angle and argue for a ballistic precessing jet for this while Agudo *et al.* [65] have reported a sharp swing in jet position angle by $> 100^\circ$ within the 0.4mas (~ 1.8 pc) inner region between 2004-2006 at 43 GHz. Based on structural changes Agudo *et al.* [65] have instead argued for an erratic wobbling of the jet along with superluminal motions in non-radial directions. Cohen [85] and Britzen *et al.* [47] study of VLBA observations at 15 GHz, on the contrary, argue for a precessing jet with a period of ~ 30 -yr and ~ 22 -yr respectively. From the analysis of the ridgeline of contours, the former has argued the jet to be a rotating helix. In contrast, a reanalysis of the same by data Britzen *et al.* [47] in combination with other observations have reported additional yearly variations under the assumption that observed changes are smooth. Based on these morphological changes, Britzen *et al.* [47] have favored a precessing jet for the cause and claims that this can explain both radio and optical variations within this framework. Correlation studies between mm radio time series with other bands (optical to γ -rays) have found a strong connection between these during the high activity periods with the increased activity associated with radio-flaring in quasi-stationary features and ejection of superluminal features [86,87].

At X-ray energies, deep exposure with the *Chandra* observatory shows a curved jet with a de-projected extension of > 1 Mpc and many bright X-ray knots/hot-spots. The location of these knots are consistent with the radio ones but follow a complex brightness profile while only the bright core is visible at NIR-optical energies [4]. Claims of detection of the host galaxy, so far, is been ambiguous [88,89] but argued to have an optical-V band magnitude of 18 [90, but see [91]].

2.4. Polarization

Like the other domains of observation, in polarization too, OJ 287 exhibits frequent and high variation in the degree of linear polarization (PD) as well as electric vector polarization angle (EVPA) at radio [e.g 67,86] and optical energies [59,62,66,78]. The reported PD range spans ~ 0 -40% at optical, ~ 1.5 -20% at IR [42,78,86] and ~ 0 -30% at radio [e.g. 86] while PA changes of up to $\sim 250^\circ$ has been observed [e.g. 59,78].

A detailed study by Villforth *et al.* [57] has reported a preferred direction for optical EVPA which is consistent with the radio measurements. They successfully decomposed the EVPA variations and found that the preferred EVPA is due to the optically polarized core which is variable on timescales of a year with a chaotic jet component superimposed on it. Similar PA in radio and optical has also been reported by Sasada *et al.* [92] from the analysis of quasi-simultaneous radio and optical observations. Holmes *et al.* [42] have reported a complex variation of polarization showing variation with time as well as frequency (energy). Contrarily, close synchronous change of optical and radio polarization has also been observed [e.g. 68,93]. Though generally optical PD follows the source flux state, systematic to chaotic and then back to systematic changes in fractional Stoke polarization during high flux states has also been observed [66]. Study of EVPA time series by Cohen *et al.* [67] over 40 years, assuming smooth changes, have found four rotation reversals in EVPA: $\sim 180^\circ$ anti-clockwise swing followed by a clockwise swing by the same amount. The swings have taken place over timescales of a few weeks to a year.

3. Discussion

The observational results listed above clearly demonstrate that OJ 287 is a very dynamic BLL object with activity over vast scales and across the observational domains. Except for a few rare cases, these results, in general, appear to be random events without any connections, reflective of stochastic variations of blazars as well as the lack of a comprehensive jet theory. Additionally, it also highlights the complexity of exploring non-linear dynamics involving a multitude of scales both theoretically and observationally [e.g. 94]. The best example of this complexity in the present case can be understood from studies of source with VLBA. Agudo *et al.* [65] study of 1995–2011 radio images at 43 GHz argue for an erratic jet variation. On the contrary, an analysis of 15 GHz VLBA images between 1995–2017 by Britzen *et al.* [47] have reported a periodicity of ~ 22 -yr assuming that observed changes are smooth while Cohen [85] have argued a periodicity of ~ 30 -yr using the same 15 GHz images but between 1995–2015 and employing ridge-line contours as an observational indicator. Thus, given our current understanding of AGNs constituents, their energy-dependent emission, and observational indications of a multitude of scales, both long and short term monitoring across the EM bands is essential to unravel the various facets and the source as a whole.

As stated already, the ~ 12 -yr QPOOs has been one of the most explored features of the source. Regarding the two class of models/interpretations for the ~ 12 -yr QPOOs, the model of Lehto and Valtonen [44] which attributes the outbursts to thermal bremsstrahlung emission as a result of disk-impact, is dynamical and predictive (the timing of the outbursts). Thus, the predicted timing of the outbursts, separation between the two outbursts, optical PD (unpolarized), and outbursts' temporal profile can be compared with observations [e.g. 62,77,95]. Though it predicts the outbursts to be unpolarized, given the underlying jet emission, PD is expected to be systematically low compared to its state before the outburst. From the timing of these outbursts [61], the model derived SMBH masses are $1.83 \times 10^{10} M_{\odot}$ and $1.5 \times 10^8 M_{\odot}$ for primary and secondary respectively [62,77,96]. The extreme mass of the primary, inconsistent with estimates from other methods [e.g. 47, and references therein] is, in fact, the biggest criticism of this model. The alternative interpretation i.e. the geometrical class of models attributes the QPOs to Doppler boosted jet synchrotron emission resulting from the jet precession [e.g. 46–48,54,56]. Further, geometrical models are kinematic in the sense that they are mainly concerned with reproducing the QPOs and lack any predictive power of the timing of these outbursts. These models mainly argue the central engine mass in the range of a few $\times (10^7 - 10^9) M_{\odot}$ [47,48,56]. However, it should be noted the system mass in these models is not dynamically connected with the model parameters and have been mainly inferred or argued using other observations [47,56, and references therein]. Thus, if the geometrical interpretation is true, the outbursts should be, in general, highly polarized. Also, there should be a coherent simultaneous rise of emission across the EM spectrum with similar temporal profiles. An important caveat in this interpretation, however, is that even jet emission has been observed to show low PD during flares and thus, need statistically relevant polarization data to test either class of models. Additionally, OJ 287 being a BLL object, knowing the expected time of outburst allow a targeted observation campaign to study HE emission mechanisms – one of the focus of intense research in the blazar community in the *Fermi* era. In the context of these two, the MW observation of the 2015 outburst provides new, independent clues as argued below.

As per the prediction for the 2015 outburst in the disk-impact SBBH model [November 2015 – January 2016, 97], an outburst with the expected signature – flux peak coincident with a dip in the PD [$< 10\%$; 62,78] and broadly following the expected temporal profile of a sharp rise followed by a slower decline with multiple smaller outbursts, was observed on December 5th, 2015 [MJD: 57361; 45,62]. Additionally, a coincident large systematic swing of $\sim 200^{\circ}$ in the optical EVPA was also observed, similar to the EVPA swing during the 1994 outburst [59]. The most important point about 2015 outburst, however, was that it was the first QPOO with a true broadband coverage from radio to MeV-GeV energies, thanks to the *Fermi*. Previous observation by CGRO of the 1994 outburst only claimed a probable detection in a “hard state” without any spectral study [75] while 2007 observations by the VHE facility MAGIC resulted in only upper limit [30]. A detailed systematic study of broadband

activity around the 2015 QPOO by Kushwaha *et al.* [60] reported rise/outburst at X-ray and MeV-GeV energies as well. The observed MW variations were typical of the source, showed simultaneous variability from NIR to γ -ray energies [60] but broadband SEDs revealed a new spectral state of the source characterized by a break in the NIR-optical SED and a hardening of MeV-GeV emission with a shift in its peak emission. Further spectrottemporal analyses revealed that the NIR-optical break first appeared on 27 May 2013 (MJD 56439) within the available NIR-optical data and is fairly well constrained in the sense that records just before this i.e. MJD 56434 and before do not show such spectral break. It should, however, be noted that the data gaps before and after MJD 56439 do not allow to track the spectral evolution, which on first sight appears as though the spectral break is due to drop of the two data points (J & K bands; ref fig. 1-c). In fact, a power-law spectrum from these two data points already hints a marginal excess even before MJD 56439 but is unreliable given that low-energy hump peaks near these energies which may wash out the intrinsic spectrum due to smoothing by change in spectral shape.

As for spectral changes and HE emission is concerned, multiple explanations have been proposed. Kushwaha *et al.* [60] showed that an EC-BLR reproduces the MeV-GeV emission while NIR-optical break nicely fits the description of a standard disk emission of a $\sim 10^{10} M_{\odot}$ SMBH (ref 1-(b)). Subsequently, Qian [98] argued that NIR-optical break is actually a shift in synchrotron peak and is in tune with the shift observed in HE SED peak while Oikonomou *et al.* [99] has proposed a hadronic scenario for the MeV-GeV. However, as shown in Kushwaha *et al.* [100], the SED corresponding to the impact flare has similar NIR and X-ray emission and lacks any spectral change vis-a-vis 2009 jet SEDs [28]. This rules out Qian [98] interpretation and also the previous EC-IR explanation for the MeV-GeV emission [100]. The hadronic model, on the other hand, mainly focuses on the interpretation of the MeV-GeV emission and the NIR-optical break remains unexplained. Neither the optically thin bremsstrahlung emission from a 25eV thermal plasma responsible for QPOOs, as argued in Valtonen *et al.* [101] is consistent with the NIR-optical break though it may have a sub-dominant contribution. Optically thin bremsstrahlung emissivity has a spectral index of ~ 0 ($F_{\nu} \sim \nu^{-a}$). Thus, in the blazar SED representation (νF_{ν}) it will have a spectral index of ~ -1 , contrary (rising) to the observed optical-UV (declining) SED [see 96]. At most, the maximum possible contribution can be the lowest flux value observed in the NIR-UV bands i.e. UVOT-w2 band (1.5×10^{15} Hz). With this, the flux contribution at NIR-optical junction ($\sim 10^{14}$ Hz) will be an order of magnitude below the UVOT-w2 band, contrary to the observed SED (see 1-(b)). Further, for IC, bremsstrahlung (and accretion-disk) photons energy density will appear de-boosted by a factor of the square of the bulk Lorentz factor (Γ) of the emission region. Also, the IC spectrum peak (ν_p) will be at $\nu_p = \delta / (1+z) \gamma_b^2 (\nu^* / \Gamma)$ where δ is the Doppler factor, γ_b is the Lorentz factor corresponding to the break in a broken power-law particle distribution normally assumed to model blazars SEDs, z is the source redshift, and ν^* is the frequency at which the seed photon spectrum peaks [e.g. 28]. Using $\nu^* \sim 7.2 \times 10^{15}$ Hz from Pihajoki [eq 68; 95] results $\nu_p \sim 2.2 \times 10^{22}$ Hz assuming $\delta = \Gamma$ and $\gamma_b = 2000$ [28,60] while the observed HE SED peak is at $\sim 10^{24}$ Hz [60]. An additional clue against a dominant contribution of bremsstrahlung photons in IC is that the MeV-GeV spectral profile remains as it was during the 2015 QPOO [27] even after the disappearance of the NIR-optical spectral break around March 3, 2016 (MJD 57455; fig. 1-(d)).

Among the discussed HE emission mechanisms, the EC-BLR explanation seems the best description in the view of the observational records in the literature during the previous QPOOs. The interpretation is consistent with the detection of broad emission lines during the previous cycles (1984, 2005-2008) of the ~ 12 -yr optical outbursts as well as the strong changes observed in its level of emission [102]. Thus, if we combine the current EC-BLR origin of MeV-GeV emission [60] with the previous EC-IR [28] and the inability of SSC to reproduce the X-ray and γ -ray emission [28,30], these results imply that in OJ 287 the MeV-GeV emission is due to EC, both on long and short timescales. Additionally, this also provides the first clear observational evidence on the ongoing debate of the location of the blazar zone at sub-parsec and parsec scales. Further, if we extrapolate current inferences

of OJ 287 HE emission with inferences from the modeling of neutrino event SEDs of blazar TXS 0506+056 [26], it seems that MeV-GeV emission in all blazars is likely IC in origin i.e. leptonic in origin.

The 2015 QPOO was followed by yet another new and peculiar MW activity, as reported in detail by Kushwaha *et al.* [27]. It started almost immediately after the settling of the activity associated with the December 2015 outburst. The source was found to be in a historic high state in X-rays and was concurrently detected at VHEs [69]. The systematic study of broadband SEDs presented by Kushwaha *et al.* [27] established this to the presence of an additional HBL emission component with the low-energy component peak in UV-soft-X-ray region. They further showed that the broadband SEDs are broadly consistent with a two-zone leptonic model with one emitting the typical OJ 287 emission with the modified MeV-GeV spectrum and the other an HBL spectrum. An important aspect during this activity was the further hardening of the MeV-GeV gamma-ray spectrum compared to the previous December 2015 activity and also a change of fraction polarization from systematic to chaotic and then back to systematic trends [66].

The interpretation of the NIR-spectral break with an accretion disk emission has direct implications on the ongoing debate over the central engine of OJ 287. The consistency of the spectral break with an accretion disk spectrum of a $\sim 10^{10} M_{\odot}$ SMBH provides independent evidence from the energy-spectrum domain in favor of the disk impact SBBH model which is based solely on the QPOOs timing [62]. Additional strong evidence in its favor is the close coincidence between the time of appearance of the spectral break in May 2013 (MJD 56439) and the impact time predicted by the model in the SMBH frame [77]. This is in stark contrast with the geometrical class of models which argue for a total system-mass in the range of $\times (10^7 - 10^9) M_{\odot}$. However, the geometrical models are still plausible as the system-mass is not dynamically related to the model parameters. Thus, precessing jet models with a total central-engine mass of $\sim 10^{10} M_{\odot}$ are still consistent with the currently available data/results [60] in the view of the lack of statistically relevant polarization information. The biggest challenge with geometrical models, however, is their failure to explain the sharpness of the outbursts [45]. Thus, if the geometrical interpretation represents the real physics behind the phenomena, the sharpness of profile during the recurring outbursts would indicate some special physical processes happening during these repeating outbursts [e.g. 48]. Another result contrary to the geometrical class of models is the lack of similar temporal profile at radio and optical [47].

The peculiarity and uniqueness of the ~ 12 -yr QPOOs are further supported by the X-ray records in the literature during and around these outbursts. Though the concurrent NIR-optical observations during the previous cycles of ~ 12 -yr QPOOs do not show any spectral break [39,59,71], an extremely soft X-ray spectral state seems to be a generic feature within the limits of observational records. It seems to be present within a few years around these optical outbursts and shows strong variations in spectral extent, strength, and the time of appearance [30,73, and references therein], thereby suggesting a relation between the two. The 2016–2017 MW activity showing an additional transient HBL component appears to be the continuity of this trend. The peculiarity of these QPOOs is also noted from time series analysis [47]. Finally, it should be noted that all the models are primarily based on the observed periodicity and none currently reproduce all the observational features seen during these outbursts [e.g. 51]. The disk-impact model lacks proper accounting of magnetic field effects which is essential for polarization properties. Though the phenomenological interpretation for the observed PD during the 2015 outburst in Valtonen *et al.* [62] seems justified, it lacks the explanation of the large systematic EVPA swing.

4. Summary

The new spectral features seen during the 2015–2017 MW high activity of OJ 287 have provided some tantalizing, independent clues in settling two of the active ongoing debates on the source related to its central engine and MeV – GeV emission mechanism. Though different interpretations may be possible, the spectral coincidence of the NIR-optical spectral break with a standard accretion-disk emission of a $\sim 10^{10} M_{\odot}$ SMBH and its first appearance in close coincidence with the impact time

predicted by the disk-impact binary SMBH model in SMBH frame support/favor the disk-impact binary SMBH model over the geometrical class of models. However, geometrical models still cannot be ruled out confidently as the mass of the central engine is not dynamically tied with the model parameters and hence, are still plausible within the limits of currently available observational data. In this case, the sharpness of QPOOs, as well as non-similarity of optical and radio time series need an explanation. Future observations of these outbursts, particularly the duration between the twin outbursts and polarization hold the key to break this degeneracy.

Similarly, the change of the MeV-GeV spectrum is reproduced by both hadronic and leptonic scenarios. The leptonic scenario via EC-BLR, however, seems natural, consistent with the detection of broad emission lines during the previous impact duration and strong changes in its luminosity [102]. This with the inferences from the systematic broadband SEDs modeling during its previous activity [28] implies that in OJ 287 the MeV-GeV emission is due to EC, both on long and short timescales. These results also provide the first clear evidence on the debate of the location of the blazar emission region at parsec and sub-parsec scales. The extremely soft X-ray spectral states around the QPOOs make it an ideal target for the Cherenkov Telescope Array (CTA) – the next generation, ground-based gamma-ray observatory.

Funding: The Author acknowledges funding from FAPESP grant number 2015/13933-0.

Acknowledgments: The author thanks the anonymous referees for their thorough reports which helped in the improvement of the overall presentation.

Conflicts of Interest: The authors declare no conflict of interest.

Abbreviations

The following abbreviations are used in this manuscript:

AGNs	Active Galactic Nuclei
BLL	BL Lacartae
BLR	Broad Line Region
CTA	Cherenkov Telescope Array
EVPA	Electric vector polarization angle
FSRQ	Flat Spectrum Radio Quasar
HSP (HBL)	High-synchrotron peaked (High-frequency peaked BL Lac)
IC	Inverse Compton
ISP (IBL)	Intermediate-synchrotron peaked (Intermediate-frequency peaked BL Lac)
LSP (LBL)	Low-synchrotron peaked (Low-frequency peaked BL Lac)
MW	Multi-wavelength
NIR	Near-infrared
PD	Polarization Degree
QPO	Quasi-periodic Outburst
QPOO	Quasi-periodic Optical Outburst
SED	Spectral Energy Distribution
SMBH	Suppermassive Black Hole
VHE	Very High Energy ($E > 100$ GeV)

References

1. Abdo, A.A.; Ackermann, M.; Agudo, I.; Ajello, M.; Aller, H.D.; Aller, M.F.; Angelakis, E.; Arkharov, A.A.; Axelsson, M.; Bach, U.; Baldini, L.; Ballet, J.; Barbiellini, G.; Bastieri, D.; Baughman, B.M.; Bechtol, K.; Bellazzini, R.; Benitez, E.; Berdyugin, A.; Berenji, B.; Blandford, R.D.; Bloom, E.D.; Boettcher, M.; Bonamente, E.; Borgland, A.W.; Bregeon, J.; Brez, A.; Brigida, M.; Bruel, P.; Burnett, T.H.; Burrows, D.; Buson, S.; Caliendo, G.A.; Calzoletti, L.; Cameron, R.A.; Capalbi, M.; Caraveo, P.A.; Carosati, D.; Casandjian, J.M.; Cavazzuti, E.; Cecchi, C.; Çelik, Ö.; Charles, E.; Chaty, S.; Chekhtman, A.; Chen, W.P.; Chiang, J.; Chincarini, G.; Ciprini, S.; Claus, R.; Cohen- Tanugi, J.; Colafrancesco, S.; Cominsky, L.R.;

- Conrad, J.; Costamante, L.; Cutini, S.; D'ammendo, F.; Deitrick, R.; D'Elia, V.; Dermer, C.D.; de Angelis, A.; de Palma, F.; Digel, S.W.; Donnarumma, I.; Silva, E.d.C.e.; Drell, P.S.; Dubois, R.; Dultzin, D.; Dumora, D.; Falcone, A.; Farnier, C.; Favuzzi, C.; Fegan, S.J.; Focke, W.B.; Forné, E.; Fortin, P.; Frailis, M.; Fuhrmann, L.; Fukazawa, Y.; Funk, S.; Fusco, P.; Gómez, J.L.; Gargano, F.; Gasparrini, D.; Gehrels, N.; Germani, S.; Giebels, B.; Giglietto, N.; Giommi, P.; Giordano, F.; Giuliani, A.; Glanzman, T.; Godfrey, G.; Grenier, I.A.; Gronwall, C.; Grove, J.E.; Guillemot, L.; Guiriec, S.; Gurwell, M.A.; Hadasch, D.; Hanabata, Y.; Harding, A.K.; Hayashida, M.; Hays, E.; Healey, S.E.; Heidt, J.; Hiriart, D.; Horan, D.; Hoversten, E.A.; Hughes, R.E.; Itoh, R.; Jackson, M.S.; Jóhannesson, G.; Johnson, A.S.; Johnson, W.N.; Jorstad, S.G.; Kadler, M.; Kamae, T.; Katagiri, H.; Kataoka, J.; Kawai, N.; Kennea, J.; Kerr, M.; Kimeridze, G.; Knödseder, J.; Kocian, M.L.; Kopatskaya, E.N.; Koptelova, E.; Konstantinova, T.S.; Kovalev, Y.Y.; Kovalev, Y.A.; Kurtanidze, O.M.; Kuss, M.; Lande, J.; Larionov, V.M.; Latronico, L.; Leto, P.; Lindfors, E.; Longo, F.; Loparco, F.; Lott, B.; Lovellette, M.N.; Lubrano, P.; Madejski, G.M.; Makeev, A.; Marchegiani, P.; Marscher, A.P.; Marshall, F.; Max-Moerbeck, W.; Mazzotta, M.N.; McConville, W.; McEney, J.E.; Meurer, C.; Michelson, P.F.; Mitthumsiri, W.; Mizuno, T.; Moiseev, A.A.; Monte, C.; Monzani, M.E.; Morselli, A.; Moskalenko, I.V.; Murgia, S.; Nestoras, I.; Nilsson, K.; Nizhelsky, N.A.; Nolan, P.L.; Norris, J.P.; Nuss, E.; Ohsugi, T.; Ojha, R.; Omodei, N.; Orlando, E.; Ormes, J.F.; Osborne, J.; Ozaki, M.; Pacciani, L.; Padovani, P.; Pagani, C.; Page, K.; Paneque, D.; Panetta, J.H.; Parent, D.; Pasanen, M.; Pavlidou, V.; Pelassa, V.; Pepe, M.; Perri, M.; Pesce-Rollins, M.; Piranomonte, S.; Piron, F.; Pittori, C.; Porter, T.A.; Puccetti, S.; Rahoui, F.; Rainò, S.; Raiteri, C.; Rando, R.; Razzano, M.; Reimer, A.; Reimer, O.; Reposeur, T.; Richards, J.L.; Ritz, S.; Rochester, L.S.; Rodriguez, A.Y.; Romani, R.W.; Ros, J.A.; Roth, M.; Roustazadeh, P.; Ryde, F.; Sadrozinski, H.F.W.; Sadun, A.; Sanchez, D.; Sander, A.; Saz Parkinson, P.M.; Scargle, J.D.; Sellerholm, A.; Sgrò, C.; Shaw, M.S.; Sigua, L.A.; Siskind, E.J.; Smith, D.A.; Smith, P.D.; Spandre, G.; Spinelli, P.; Starck, J.L.; Stevenson, M.; Stratta, G.; Strickman, M.S.; Suson, D.J.; Tajima, H.; Takahashi, H.; Takahashi, T.; Takalo, L.O.; Tanaka, T.; Thayer, J.B.; Thayer, J.G.; Thompson, D.J.; Tibaldo, L.; Torres, D.F.; Tosti, G.; Tramacere, A.; Uchiyama, Y.; Usher, T.L.; Vasileiou, V.; Verrecchia, F.; Vilchez, N.; Villata, M.; Vitale, V.; Waite, A.P.; Wang, P.; Winer, B.L.; Wood, K.S.; Ylinen, T.; Zensus, J.A.; Zhekanis, G.V.; Ziegler, M. The Spectral Energy Distribution of Fermi Bright Blazars. *ApJ* **2010**, *716*, 30–70, [[arXiv:astro-ph.CO/0912.2040](https://arxiv.org/abs/astro-ph.CO/0912.2040)]. doi:10.1088/0004-637X/716/1/30.
2. Goyal, A.; Stawarz, Ł.; Zola, S.; Marchenko, V.; Soida, M.; Nilsson, K.; Ciprini, S.; Baran, A.; Ostrowski, M.; Wiita, P.J.; Gopal-Krishna.; Siemiginowska, A.; Sobolewska, M.; Jorstad, S.; Marscher, A.; Aller, M.F.; Aller, H.D.; Hovatta, T.; Caton, D.B.; Reichart, D.; Matsumoto, K.; Sadakane, K.; Gazeas, K.; Kidger, M.; Piirola, V.; Jermak, H.; Alicavus, F.; Baliyan, K.S.; Baransky, A.; Berdyugin, A.; Blay, P.; Boumis, P.; Boyd, D.; Bufan, Y.; Campas Torrent, M.; Campos, F.; Carrillo Gómez, J.; Dalessio, J.; Debski, B.; Dimitrov, D.; Drozd, M.; Er, H.; Erdem, A.; Escartin Pérez, A.; Fallah Ramazani, V.; Filippenko, A.V.; Gafton, E.; Garcia, F.; Godunova, V.; Gómez Pinilla, F.; Gopinathan, M.; Haislip, J.B.; Haque, S.; Harmanen, J.; Hudec, R.; Hurst, G.; Ivarsen, K.M.; Joshi, A.; Kagitani, M.; Karaman, N.; Karjalainen, R.; Kaur, N.; Koziel-Wierzbowska, D.; Kuligowska, E.; Kundera, T.; Kurowski, S.; Kvammen, A.; LaCluyze, A.P.; Lee, B.C.; Liakos, A.; Lozano de Haro, J.; Moore, J.P.; Mugrauer, M.; Naves Noguez, R.; Neely, A.W.; Ogloza, W.; Okano, S.; Pajdosz, U.; Pandey, J.C.; Perri, M.; Poyner, G.; Provencal, J.; Pursimo, T.; Raj, A.; Rajkumar, B.; Reinthal, R.; Reynolds, T.; Saario, J.; Sadegi, S.; Sakanoi, T.; Salto González, J.L.; Sameer.; Simon, A.O.; Siwak, M.; Schweyer, T.; Soldán Alfaro, F.C.; Sonbas, E.; Strobl, J.; Takalo, L.O.; Tremosa Espasa, L.; Valdes, J.R.; Vasylenko, V.V.; Verrecchia, F.; Webb, J.R.; Yoneda, M.; Zejmo, M.; Zheng, W.; Zielinski, P.; Janik, J.; Chavushyan, V.; Mohammed, I.; Cheung, C.C.; Giroletti, M. Stochastic Modeling of Multiwavelength Variability of the Classical BL Lac Object OJ 287 on Timescales Ranging from Decades to Hours. *ApJ* **2018**, *863*, 175. doi:10.3847/1538-4357/aad2de.
 3. Uchiyama, Y.; Urry, C.M.; Cheung, C.C.; Jester, S.; Van Deyne, J.; Coppi, P.; Sambruna, R.M.; Takahashi, T.; Tavecchio, F.; Maraschi, L. Shedding New Light on the 3C 273 Jet with the Spitzer Space Telescope. *ApJ* **2006**, *648*, 910–921, [[astro-ph/0605530](https://arxiv.org/abs/astro-ph/0605530)]. doi:10.1086/505964.
 4. Marscher, A.P.; Jorstad, S.G. The Megaparsec-scale X-ray Jet of The BL Lac Object OJ287. *ApJ* **2011**, *729*, 26, [[arXiv:astro-ph.CO/1008.5178](https://arxiv.org/abs/astro-ph.CO/1008.5178)]. doi:10.1088/0004-637X/729/1/26.
 5. Urry, C.M.; Padovani, P. Unified Schemes for Radio-Loud Active Galactic Nuclei. *PASP* **1995**, *107*, 803, [[astro-ph/9506063](https://arxiv.org/abs/astro-ph/9506063)]. doi:10.1086/133630.
 6. Atwood, W.B.; Abdo, A.A.; Ackermann, M.; Althouse, W.; Anderson, B.; Axelsson, M.; Baldini, L.; Ballet, J.; Band, D.L.; Barbiellini, G.; Bartelt, J.; Bastieri, D.; Baughman, B.M.; Bechtol, K.; Bédérède, D.; Bellardi, F.;

- Bellazzini, R.; Berenji, B.; Bignami, G.F.; Bisello, D.; Bissaldi, E.; Blandford, R.D.; Bloom, E.D.; Bogart, J.R.; Bonamente, E.; Bonnell, J.; Borgland, A.W.; Bouvier, A.; Bregeon, J.; Brez, A.; Brigida, M.; Bruel, P.; Burnett, T.H.; Busetto, G.; Caliendo, G.A.; Cameron, R.A.; Caraveo, P.A.; Carius, S.; Carlson, P.; Casandjian, J.M.; Cavazzuti, E.; Ceccanti, M.; Cecchi, C.; Charles, E.; Chekhtman, A.; Cheung, C.C.; Chiang, J.; Chipaux, R.; Cillis, A.N.; Ciprini, S.; Claus, R.; Cohen-Tanugi, J.; Condamore, S.; Conrad, J.; Corbet, R.; Corucci, L.; Costamante, L.; Cutini, S.; Davis, D.S.; Decotigny, D.; DeKlotz, M.; Dermer, C.D.; de Angelis, A.; Digel, S.W.; do Couto e Silva, E.; Drell, P.S.; Dubois, R.; Dumora, D.; Edmonds, Y.; Fabiani, D.; Farnier, C.; Favuzzi, C.; Flath, D.L.; Fleury, P.; Focke, W.B.; Funk, S.; Fusco, P.; Gargano, F.; Gasparrini, D.; Gehrels, N.; Gentit, F.X.; Germani, S.; Giebels, B.; Giglietto, N.; Giommi, P.; Giordano, F.; Glanzman, T.; Godfrey, G.; Grenier, I.A.; Grondin, M.H.; Grove, J.E.; Guillemot, L.; Guiriec, S.; Haller, G.; Harding, A.K.; Hart, P.A.; Hays, E.; Healey, S.E.; Hirayama, M.; Hjalmarsdotter, L.; Horn, R.; Hughes, R.E.; Jóhannesson, G.; Johansson, G.; Johnson, A.S.; Johnson, R.P.; Johnson, T.J.; Johnson, W.N.; Kamae, T.; Katagiri, H.; Kataoka, J.; Kavelaars, A.; Kawai, N.; Kelly, H.; Kerr, M.; Klamra, W.; Knödseder, J.; Kocian, M.L.; Komin, N.; Kuehn, F.; Kuss, M.; Landriu, D.; Latronico, L.; Lee, B.; Lee, S.H.; Lemoine-Goumard, M.; Lionetto, A.M.; Longo, F.; Loparco, F.; Lott, B.; Lovellette, M.N.; Lubrano, P.; Madejski, G.M.; Makeev, A.; Marangelli, B.; Massai, M.M.; Mazziotta, M.N.; McEnery, J.E.; Menon, N.; Meurer, C.; Michelson, P.F.; Minuti, M.; Mirizzi, N.; Mitthumsiri, W.; Mizuno, T.; Moiseev, A.A.; Monte, C.; Monzani, M.E.; Moretti, E.; Morselli, A.; Moskalenko, I.V.; Murgia, S.; Nakamori, T.; Nishino, S.; Nolan, P.L.; Norris, J.P.; Nuss, E.; Ohno, M.; Ohsugi, T.; Omodei, N.; Orlando, E.; Ormes, J.F.; Paccagnella, A.; Paneque, D.; Panetta, J.H.; Parent, D.; Pearce, M.; Pepe, M.; Perazzo, A.; Pesce-Rollins, M.; Picozza, P.; Pieri, L.; Pinchera, M.; Piron, F.; Porter, T.A.; Poupard, L.; Rainò, S.; Rando, R.; Rapposelli, E.; Razzano, M.; Reimer, A.; Reimer, O.; Reposeur, T.; Reyes, L.C.; Ritz, S.; Rochester, L.S.; Rodriguez, A.Y.; Romani, R.W.; Roth, M.; Russell, J.J.; Ryde, F.; Sabatini, S.; Sadrozinski, H.F.W.; Sanchez, D.; Sand, A.; Sapozhnikov, L.; Parkinson, P.M.S.; Scargle, J.D.; Schalk, T.L.; Scolieri, G.; Sgrò, C.; Share, G.H.; Shaw, M.; Shimokawabe, T.; Shrader, C.; Sierpowska-Bartosik, A.; Siskind, E.J.; Smith, D.A.; Smith, P.D.; Spandre, G.; Spinelli, P.; Starck, J.L.; Stephens, T.E.; Strickman, M.S.; Strong, A.W.; Suson, D.J.; Tajima, H.; Takahashi, H.; Takahashi, T.; Tanaka, T.; Tenze, A.; Tether, S.; Thayer, J.B.; Thayer, J.G.; Thompson, D.J.; Tibaldo, L.; Tibolla, O.; Torres, D.F.; Tosti, G.; Tramacere, A.; Turri, M.; Usher, T.L.; Vilchez, N.; Vitale, V.; Wang, P.; Watters, K.; Winer, B.L.; Wood, K.S.; Ylinen, T.; Ziegler, M. The Large Area Telescope on the Fermi Gamma-Ray Space Telescope Mission. *ApJ* **2009**, *697*, 1071–1102, [[arXiv:astro-ph/0902.1089](https://arxiv.org/abs/astro-ph/0902.1089)]. doi:10.1088/0004-637X/697/2/1071.
7. The Fermi-LAT collaboration. Fermi Large Area Telescope Fourth Source Catalog. *arXiv e-prints* **2019**, p. arXiv:1902.10045, [[arXiv:astro-ph/1902.10045](https://arxiv.org/abs/astro-ph/1902.10045)].
 8. Kushwaha, P.; Sinha, A.; Misra, R.; Singh, K.P.; de Gouveia Dal Pino, E.M. Gamma-Ray Flux Distribution and Nonlinear Behavior of Four LAT Bright AGNs. *ApJ* **2017**, *849*, 138, [[arXiv:astro-ph/1709.07904](https://arxiv.org/abs/astro-ph/1709.07904)]. doi:10.3847/1538-4357/aa8ef5.
 9. Kushwaha, P.; Chandra, S.; Misra, R.; Sahayanathan, S.; Singh, K.P.; Baliyan, K.S. Evidence for Two Lognormal States in Multi-wavelength Flux Variation of FSRQ PKS 1510-089. *ApJL* **2016**, *822*, L13, [[arXiv:astro-ph/1604.04335](https://arxiv.org/abs/astro-ph/1604.04335)]. doi:10.3847/2041-8205/822/1/L13.
 10. Scaringi, S.; Maccarone, T.J.; Kording, E.; Knigge, C.; Vaughan, S.; Marsh, T.R.; Aranzana, E.; Dhillon, V.S.; Barros, S.C.C. Accretion-induced variability links young stellar objects, white dwarfs, and black holes. *Science Advances* **2015**, *1*, e1500686–e1500686. doi:10.1126/sciadv.1500686.
 11. Gupta, A.C.; Tripathi, A.; Wiita, P.J.; Kushwaha, P.; Zhang, Z.; Bambi, C. Detection of a quasi-periodic oscillation in γ -ray light curve of the high-redshift blazar B2 1520+31. *MNRAS* **2019**, *484*, 5785–5790, [[arXiv:astro-ph/1810.12607](https://arxiv.org/abs/astro-ph/1810.12607)]. doi:10.1093/mnras/stz395.
 12. Fossati, G.; Maraschi, L.; Celotti, A.; Comastri, A.; Ghisellini, G. A unifying view of the spectral energy distributions of blazars. *MNRAS* **1998**, *299*, 433–448, [[astro-ph/9804103](https://arxiv.org/abs/astro-ph/9804103)]. doi:10.1046/j.1365-8711.1998.01828.x.
 13. Boettcher, M.; Harris, D.E.; Krawczynski, H. *Relativistic Jets from Active Galactic Nuclei*; 2012.
 14. Böttcher, M.; Reimer, A.; Sweeney, K.; Prakash, A. Leptonic and Hadronic Modeling of Fermi-detected Blazars. *ApJ* **2013**, *768*, 54, [[arXiv:astro-ph/1304.0605](https://arxiv.org/abs/astro-ph/1304.0605)]. doi:10.1088/0004-637X/768/1/54.
 15. Zdziarski, A.A.; Böttcher, M. Hadronic models of blazars require a change of the accretion paradigm. *MNRAS* **2015**, *450*, L21–L25. doi:10.1093/mnras/15039.

16. Ghisellini, G.; Tavecchio, F. The blazar sequence: a new perspective. *MNRAS* **2008**, *387*, 1669–1680, [[arXiv:astro-ph/0802.1918](#)]. doi:10.1111/j.1365-2966.2008.13360.x.
17. Ghisellini, G.; Tavecchio, F.; Maraschi, L.; Celotti, A.; Sbarrato, T. The power of relativistic jets is larger than the luminosity of their accretion disks. *Nature* **2014**, *515*, 376–378, [[arXiv:astro-ph.HE/1411.5368](#)]. doi:10.1038/nature13856.
18. Albert, J.; Aliu, E.; Anderhub, H.; Antoranz, P.; Armada, A.; Baixeras, C.; Barrio, J.A.; Bartko, H.; Bastieri, D.; Becker, J.K.; Bednarek, W.; Berger, K.; Bigongiari, C.; Biland, A.; Bock, R.K.; Bordas, P.; Bosch-Ramon, V.; Bretz, T.; Britvitch, I.; Camara, M.; Carmona, E.; Chilingarian, A.; Coarasa, J.A.; Commichau, S.; Contreras, J.L.; Cortina, J.; Costado, M.T.; Curtef, V.; Danielyan, V.; Dazzi, F.; De Angelis, A.; Delgado, C.; de los Reyes, R.; De Lotto, B.; Domingo-Santamaría, E.; Dorner, D.; Doro, M.; Errando, M.; Fagiolini, M.; Ferenc, D.; Fernández, E.; Firpo, R.; Flix, J.; Fonseca, M.V.; Font, L.; Fuchs, M.; Galante, N.; García-López, R.J.; Garczarczyk, M.; Gaug, M.; Giller, M.; Goebel, F.; Hakobyan, D.; Hayashida, M.; Hengstebeck, T.; Herrero, A.; Höhne, D.; Hose, J.; Hrupec, D.; Hsu, C.C.; Jacon, P.; Jogler, T.; Kosyra, R.; Kranich, D.; Kritzer, R.; Laille, A.; Lindfors, E.; Lombardi, S.; Longo, F.; López, J.; López, M.; Lorenz, E.; Majumdar, P.; Maneva, G.; Mannheim, K.; Mansutti, O.; Mariotti, M.; Martínez, M.; Mazin, D.; Merck, C.; Meucci, M.; Meyer, M.; Miranda, J.M.; Mirzoyan, R.; Mizobuchi, S.; Moralejo, A.; Nieto, D.; Nilsson, K.; Ninkovic, J.; Oña-Wilhelmi, E.; Otte, N.; Oya, I.; Paneque, D.; Panniello, M.; Paoletti, R.; Paredes, J.M.; Pasanen, M.; Pascoli, D.; Paus, F.; Pegna, R.; Persic, M.; Peruzzo, L.; Piccioli, A.; Prandini, E.; Puchades, N.; Raymers, A.; Rhode, W.; Ribó, M.; Rico, J.; Rissi, M.; Robert, A.; Rügamer, S.; Saggion, A.; Saito, T.; Sánchez, A.; Sartori, P.; Scalzotto, V.; Scapin, V.; Schmitt, R.; Schweizer, T.; Shayduk, M.; Shinozaki, K.; Shore, S.N.; Sidro, N.; Sillanpää, A.; Sobczynska, D.; Stamerra, A.; Stark, L.S.; Takalo, L.; Tavecchio, F.; Temnikov, P.; Tescaro, D.; Teshima, M.; Torres, D.F.; Turini, N.; Vankov, H.; Vitale, V.; Wagner, R.M.; Wibig, T.; Wittek, W.; Zandanel, F.; Zanin, R.; Zapatero, J. Variable Very High Energy γ -Ray Emission from Markarian 501. *ApJ* **2007**, *669*, 862–883, [[arXiv:astro-ph/astro-ph/0702008](#)]. doi:10.1086/521382.
19. Dermer, C.D.; Schlickeiser, R.; Mastichiadis, A. High-energy gamma radiation from extragalactic radio sources. *A&A* **1992**, *256*, L27–L30.
20. Sikora, M.; Begelman, M.C.; Rees, M.J. Comptonization of Diffuse Ambient Radiation by a Relativistic Jet: The Source of Gamma Rays from Blazars? *ApJ* **1994**, *421*, 153. doi:10.1086/173633.
21. Bloom, S.D.; Marscher, A.P. An Analysis of the Synchrotron Self-Compton Model for the Multi-Wave Band Spectra of Blazars. *ApJ* **1996**, *461*, 657. doi:10.1086/177092.
22. Ackermann, M.; Ajello, M.; Ballet, J.; Barbiellini, G.; Bastieri, D.; Bellazzini, R.; Blandford, R.D.; Bloom, E.D.; Bonamente, E.; Borghland, A.W.; et al.. Multi-wavelength Observations of Blazar AO 0235+164 in the 2008-2009 Flaring State. *ApJ* **2012**, *751*, 159, [[arXiv:astro-ph.HE/1207.2932](#)]. doi:10.1088/0004-637X/751/2/159.
23. IceCube Collaboration.; Aartsen, M.G.; Ackermann, M.; Adams, J.; Aguilar, J.A.; Ahlers, M.; Ahrens, M.; Samarai, I.A.; Altmann, D.; Andeen, K.; Anderson, T.; Anseau, I.; Anton, G.; Argüelles, C.; Arsioli, B.; Auffenberg, J.; Axani, S.; Bagherpour, H.; Bai, X.; Barron, J.P.; Barwick, S.W.; Baum, V.; Bay, R.; Beatty, J.J.; Becker Tjus, J.; Becker, K.H.; BenZvi, S.; Berley, D.; Bernardini, E.; Besson, D.Z.; Binder, G.; Bindig, D.; Blaufuss, E.; Blot, S.; Bohm, C.; Börner, M.; Bos, F.; Böser, S.; Botner, O.; Bourbeau, E.; Bourbeau, J.; Bradascio, F.; Braun, J.; Brenzke, M.; Bretz, H.P.; Bron, S.; Brostean-Kaiser, J.; Burgman, A.; Busse, R.S.; Carver, T.; Cheung, E.; Chirkin, D.; Christov, A.; Clark, K.; Classen, L.; Coenders, S.; Collin, G.H.; Conrad, J.M.; Coppin, P.; Correa, P.; Cowen, D.F.; Cross, R.; Dave, P.; Day, M.; de André, J.P.A.M.; De Clercq, C.; DeLaunay, J.J.; Dembinski, H.; DeRidder, S.; Desiati, P.; de Vries, K.D.; de Wasseige, G.; de With, M.; DeYoung, T.; Díaz-Vélez, J.C.; di Lorenzo, V.; Dujmovic, H.; Dumm, J.P.; Dunkman, M.; Dvorak, E.; Eberhardt, B.; Ehrhardt, T.; Eichmann, B.; Eller, P.; Evenson, P.A.; Fahey, S.; Fazely, A.R.; Felde, J.; Filimonov, K.; Finley, C.; Flis, S.; Franckowiak, A.; Friedman, E.; Fritz, A.; Gaisser, T.K.; Gallagher, J.; Gerhardt, L.; Ghorbani, K.; Giommi, P.; Glauch, T.; Glüsenkamp, T.; Goldschmidt, A.; Gonzalez, J.G.; Grant, D.; Griffith, Z.; Haack, C.; Hallgren, A.; Halzen, F.; Hanson, K.; Hebecker, D.; Heereman, D.; Helbing, K.; Hellauer, R.; Hickford, S.; Hignight, J.; Hill, G.C.; Hoffman, K.D.; Hoffmann, R.; Hoinka, T.; Hokanson-Fasig, B.; Hoshina, K.; Huang, F.; Huber, M.; Hultqvist, K.; Hünnefeld, M.; Hussain, R.; In, S.; Iovine, N.; Ishihara, A.; Jacobi, E.; Japaridze, G.S.; Jeong, M.; Jero, K.; Jones, B.J.P.; Kalaczynski, P.; Kang, W.; Kappes, A.; Kappesser, D.; Karg, T.; Karle, A.; Katz, U.; Kauer, M.; Keivani, A.; Kelley, J.L.; Kheirandish, A.; Kim, J.; Kim, M.; Kintscher, T.; Kiryluk, J.; Kittler, T.; Klein, S.R.; Koirala, R.; Kolanoski, H.;

- Köpke, L.; Kopper, C.; Kopper, S.; Koschinsky, J.P.; Koskinen, D.J.; Kowalski, M.; Krammer, B.; Krings, K.; Kroll, M.; Krückl, G.; Kunwar, S.; Kurahashi, N.; Kuwabara, T.; Kyriacou, A.; Labare, M.; Lanfranchi, J.L.; Larson, M.J.; Lauber, F.; Leonard, K.; Lesiak-Bzdak, M.; Leuermann, M.; Liu, Q.R.; Lozano Mariscal, C.J.; Lu, L.; Lünemann, J.; Luszczak, W.; Madsen, J.; Maggi, G.; Mahn, K.B.M.; Mancina, S.; Maruyama, R.; Mase, K.; Maunu, R.; Meagher, K.; Medici, M.; Meier, M.; Menne, T.; Merino, G.; Meures, T.; Miarecki, S.; Micallef, J.; Momenté, G.; Montaruli, T.; Moore, R.W.; Morse, R.; Moulai, M.; Nahnauer, R.; Nakarmi, P.; Naumann, U.; Neer, G.; Niederhausen, H.; Nowicki, S.C.; Nygren, D.R.; Obertacke Pollmann, A.; Olivas, A.; O’Murchadha, A.; O’Sullivan, E.; Padovani, P.; Palczewski, T.; Pandya, H.; Pankova, D.V.; Peiffer, P.; Pepper, J.A.; Pérez de los Heros, C.; Pieloth, D.; Pinat, E.; Plum, M.; Price, P.B.; Przybylski, G.T.; Raab, C.; Rädcl, L.; Rameez, M.; Rawlins, K.; Rea, I.C.; Reimann, R.; Relethford, B.; Relich, M.; Resconi, E.; Rhode, W.; Richman, M.; Robertson, S.; Rongen, M.; Rott, C.; Ruhe, T.; Ryckbosch, D.; Rysewyk, D.; Safa, I.; Sahakyan, N.; Sälzer, T.; Sanchez Herrera, S.E.; Sandrock, A.; Sandroos, J.; Santander, M.; Sarkar, S.; Sarkar, S.; Satalecka, K.; Schlunder, P.; Schmidt, T.; Schneider, A.; Schoenen, S.; Schöneberg, S.; Schumacher, L.; Sclafani, S.; Seckel, D.; Seunarine, S.; Soedingrekso, J.; Soldin, D.; Song, M.; Spiczak, G.M.; Spiering, C.; Stachurska, J.; Stamatikos, M.; Stanev, T.; Stasik, A.; Stettner, J.; Steuer, A.; Stezelberger, T.; Stokstad, R.G.; Stöbl, A.; Strotjohann, N.L.; Stuttard, T.; Sullivan, G.W.; Sutherland, M.; Taboada, I.; Tatar, J.; Tenholt, F.; Ter-Antonyan, S.; Terliuk, A.; Tilav, S.; Toale, P.A.; Tobin, M.N.; Toennis, C.; Toscano, S.; Tosi, D.; Tselengidou, M.; Tung, C.F.; Turcati, A.; Turley, C.F.; Ty, B.; Unger, E.; Usner, M.; Vandenbroucke, J.; Van Driessche, W.; van Eijk, D.; van Eijndhoven, N.; Vanheule, S.; van Santen, J.; Vogel, E.; Vraeghe, M.; Walck, C.; Wallace, A.; Wallraff, M.; Wandler, F.D.; Wandkowsky, N.; Waza, A.; Weaver, C.; Weiss, M.J.; Wendt, C.; Werthebach, J.; Westerhoff, S.; Whelan, B.J.; Whitehorn, N.; Wiebe, K.; Wiebusch, C.H.; Wille, L.; Williams, D.R.; Wills, L.; Wolf, M.; Wood, J.; Wood, T.R.; Woschnagg, K.; Xu, D.L.; Xu, X.W.; Xu, Y.; Yanez, J.P.; Yodh, G.; Yoshida, S.; Yuan, T. Neutrino emission from the direction of the blazar TXS 0506+056 prior to the IceCube-170922A alert. *Science* **2018**, *361*, 147–151. doi:10.1126/science.aat2890.
24. IceCube Collaboration.; Aartsen, M.G.; Ackermann, M.; Adams, J.; Aguilar, J.A.; Ahlers, M.; Ahrens, M.; Al Samarai, I.; Altmann, D.; Andeen, K.; et al.. Multimessenger observations of a flaring blazar coincident with high-energy neutrino IceCube-170922A. *Science* **2018**, *361*, eaat1378, [arXiv:astro-ph.HE/1807.08816]. doi:10.1126/science.aat1378.
25. Murase, K.; Bartos, I. High-Energy Multi-Messenger Transient Astrophysics. *arXiv e-prints* **2019**, p. arXiv:1907.12506, [arXiv:astro-ph.HE/1907.12506].
26. Gao, S.; Fedynitch, A.; Winter, W.; Pohl, M. Modelling the coincident observation of a high-energy neutrino and a bright blazar flare. *Nature Astronomy* **2018**, p. 154. doi:10.1038/s41550-018-0610-1.
27. Kushwaha, P.; Gupta, A.C.; Wiita, P.J.; Pal, M.; Gaur, H.; de Gouveia Dal Pino, E.M.; Kurtanidze, O.M.; Semkov, E.; Damjanovic, G.; Hu, S.M.; Uemura, M.; Vince, O.; Darriba, A.; Gu, M.F.; Bachev, R.; Chen, X.; Itoh, R.; Kawabata, M.; Kurtanidze, S.O.; Nakaoka, T.; Nikolashvili, M.G.; Sigua, L.A.; Strigachev, A.; Zhang, Z. The ever-surprising blazar OJ 287: multiwavelength study and appearance of a new component in X-rays. *MNRAS* **2018**, *479*, 1672–1684, [arXiv:astro-ph.HE/1803.10213]. doi:10.1093/mnras/sty1499.
28. Kushwaha, P.; Sahayanathan, S.; Singh, K.P. High energy emission processes in OJ 287 during 2009 flare. *MNRAS* **2013**, *433*, 2380–2388, [arXiv:astro-ph.HE/1305.5065]. doi:10.1093/mnras/stt904.
29. Arsioli, B.; Chang, Y.L. The γ -ray emitting region in low synchrotron peak blazars. Testing self-synchrotron Compton and external Compton scenarios. *A&A* **2018**, *616*, A63. doi:10.1051/0004-6361/201833005.
30. Seta, H.; Isobe, N.; Tashiro, M.S.; Yaji, Y.; Arai, A.; Fukuhara, M.; Kohno, K.; Nakanishi, K.; Sasada, M.; Shimajiri, Y.; Tosaki, T.; Uemura, M.; Anderhub, H.; Antonelli, L.A.; Antoranz, P.; Backes, M.; Baixeras, C.; Balestra, S.; Barrio, J.A.; Bastieri, D.; Becerra González, J.; Becker, J.K.; Bednarek, W.; Berger, K.; Bernardini, E.; Biland, A.; Bock, R.K.; Bonnoli, G.; Bordas, P.; Borla Tridon, D.; Bosch-Ramon, V.; Bose, D.; Braun, I.; Bretz, T.; Britvitch, I.; Camara, M.; Carmona, E.; Commichau, S.; Contreras, J.L.; Cortina, J.; Costado Dios, M.T.; Covino, S.; Curtef, V.; Dazzi, F.; de Angelis, A.; de Cea Del Pozo, E.; de Los Reyes, R.; de Lotto, B.; de Maria, M.; de Sabata, F.; Delgado Méndez, C.; Domínguez, A.; Dorner, D.; Doro, M.; Elsaesser, D.; Errando, M.; Ferenc, D.; Fernández, E.; Firpo, R.; Fonseca, M.V.; Font, L.; Galante, N.; García López, R.J.; Garczarczyk, M.; Gaug, M.; Goebel, F.; Hadasch, D.; Hayashida, M.; Herrero, A.; Hildebrand, D.; Höhne-Mönch, D.; Hose, J.; Hsu, C.C.; Jogler, T.; Kranich, D.; La Barbera, A.; Laille, A.; Leonardo, E.; Lindfors, E.; Lombardi, S.; Longo, F.; López, D.; Lorenz, E.; Majumdar, P.; Maneva, G.; Mankuzhiyil, N.; Mannheim, K.; Maraschi, L.; Mariotti, M.; Martínez, M.; Mazin, D.; Meucci, M.; Meyer, M.; Miguel Miranda, J.; Mirzoyan, R.; Miyamoto,

- H.; Moldón, J.; Moles, M.; Moralejo, A.; Nieto, D.; Nilsson, K.; Ninkovic, J.; Otte, N.; Oya, I.; Paoletti, R.; Paredes, J.M.; Pasanen, M.; Pascoli, D.; Pauss, F.; Pegna, R.G.; Perez-Torres, M.A.; Persic, M.; Peruzzo, L.; Prada, F.; Prandini, E.; Puchades, N.; Reichardt, I.; Rhode, W.; Ribó, M.; Rico, J.; Rissi, M.; Robert, A.; Rügamer, S.; Saggion, A.; Saito, T.Y.; Salvati, M.; Sánchez-Conde, M.; Satalecka, K.; Scalzotto, V.; Scapin, V.; Schweizer, T.; Shayduk, M.; Shore, S.N.; Sidro, N.; Sierpowska-Bartosik, A.; Sillanpää, A.; Sitarek, J.; Sobczynska, D.; Spanier, F.; Stamerra, A.; Stark Schneebeli, L.S.; Takalo, L.; Tavecchio, F.; Temnikov, P.; Tesaro, D.; Teshima, M.; Tluczykont, M.; Torres, D.F.; Turini, N.; Vankov, H.; Wagner, R.M.; Wittek, W.; Zabalza, V.; Zandanel, F.; Zanin, R.; Zapatero, J. Suzaku and Multi-Wavelength Observations of OJ 287 during the Periodic Optical Outburst in 2007. *Publications of the Astronomical Society of Japan* **2009**, *61*, 1011, [[arXiv:astro-ph.CO/0906.0234](https://arxiv.org/abs/astro-ph.CO/0906.0234)]. doi:10.1093/pasj/61.5.1011.
31. Costamante, L.; Cutini, S.; Tosti, G.; Antolini, E.; Tramacere, A. On the origin of gamma-rays in Fermi blazars: beyond the broad-line region. *MNRAS* **2018**, *477*, 4749–4767. doi:10.1093/mnras/sty887.
 32. Dickel, J.R.; Yang, K.S.; McVittie, G.C.; Swenson, Jr., G.W. A survey of the sky at 610.5 MHz. II. The region between declinations +15 and +22 degrees. *AJ* **1967**, *72*, 757–768. doi:10.1086/110305.
 33. Blake, G.M. Observations of Extragalactic Radio Sources Having Unusual Spectra. *ApL* **1970**, *6*, 201.
 34. Kinman, T.D.; Conklin, E.K. Observations of OJ 287 at Optical and Millimeter Wavelengths. *ApL* **1971**, *9*, 147–149.
 35. Visvanathan, N. The Spectrum of OJ 287. *ApJ* **1973**, *185*, 145–152. doi:10.1086/152404.
 36. Sitko, M.L.; Junkkarinen, V.T. Continuum and line fluxes of OJ287 at minimum light. *PASP* **1985**, *97*, 1158–1162. doi:10.1086/131679.
 37. Stickel, M.; Fried, J.W.; Kuehr, H. Optical spectroscopy of 1 Jy BL Lacertae objects and flat spectrum radio sources. *A&AS* **1989**, *80*, 103–114.
 38. Andrew, B.H.; Harvey, G.A.; Medd, W.J. OJ 287: An Exceptionally Active Variable Source. *ApL* **1971**, *9*, 151.
 39. Dyck, H.M.; Kinman, T.D.; Lockwood, G.W.; Landolt, A.U. Observations of OJ 287 between 0.36 and 3.4 μm . *Nature Physical Science* **1971**, *234*, 71–72. doi:10.1038/physci234071a0.
 40. Epstein, E.E.; Fogarty, W.G.; Hackney, K.R.; Hackney, R.L.; Leacock, R.J.; Pomphrey, R.B.; Scott, R.L.; Smith, A.G.; Hawkins, R.W.; Roeder, R.C.; Gary, B.L.; Penston, M.V.; Tritton, K.P.; Bertaud, C.; Véron, M.P.; Wlérick, G.; Bernard, A.; Bigay, J.H.; Merlin, P.; Durand, A.; Sause, G.; Becklin, E.E.; Neugebauer, G.; Wynn-Williams, C.G. 3C 120, BL Lacertae, and OJ 287: Coordinated Optical, Infrared, and Radio Observations of Intraday Variability. *ApJL* **1972**, *178*, L51. doi:10.1086/181083.
 41. Visvanathan, N.; Elliot, J.L. Variations of the radio source OJ 287 at optical wavelengths. *ApJ* **1973**, *179*, 721–730. doi:10.1086/151911.
 42. Holmes, P.A.; Brand, P.W.J.L.; Impey, C.D.; Williams, P.M.; Smith, P.; Elston, R.; Balonek, T.; Zeilik, M.; Burns, J.; Heckert, P.; Barvainis, R.; Kenny, J.; Schmidt, G.; Puschell, J. A polarization flare in OJ 287. *MNRAS* **1984**, *211*, 497–506. doi:10.1093/mnras/211.3.497.
 43. Sillanpää, A.; Haarala, S.; Valtonen, M.J.; Sundelius, B.; Byrd, G.G. OJ 287: Binary Pair of Supermassive Black Holes. *ApJ* **1988**, *325*, 628. doi:10.1086/166033.
 44. Lehto, H.J.; Valtonen, M.J. OJ 287 Outburst Structure and a Binary Black Hole Model. *ApJ* **1996**, *460*, 207. doi:10.1086/176962.
 45. Valtonen, M.J.; Lehto, H.J.; Nilsson, K.; Heidt, J.; Takalo, L.O.; Sillanpää, A.; Villforth, C.; Kidger, M.; Poyner, G.; Pursimo, T.; Zola, S.; Wu, J.H.; Zhou, X.; Sadakane, K.; Drozd, M.; Koziel, D.; Marchev, D.; Ogloza, W.; Porowski, C.; Siwak, M.; Stachowski, G.; Winiarski, M.; Hentunen, V.P.; Nissinen, M.; Liakos, A.; Dogru, S. A massive binary black-hole system in OJ287 and a test of general relativity. *Nature* **2008**, *452*, 851–853, [[0809.1280](https://arxiv.org/abs/0809.1280)]. doi:10.1038/nature06896.
 46. Katz, J.I. A Precessing Disk in OJ 287? *ApJ* **1997**, *478*, 527–529. doi:10.1086/303811.
 47. Britzen, S.; Fendt, C.; Witzel, G.; Qian, S.J.; Pashchenko, I.N.; Kurtanidze, O.; Zajacek, M.; Martinez, G.; Karas, V.; Aller, M.; Aller, H.; Eckart, A.; Nilsson, K.; Arévalo, P.; Cuadra, J.; Subroweit, M.; Witzel, A. OJ287: deciphering the ‘Rosetta stone of blazars. *MNRAS* **2018**, *478*, 3199–3219. doi:10.1093/mnras/sty1026.
 48. Qian, S. A tentative double-jet model for blazar OJ287. *arXiv e-prints* **2018**, p. arXiv:1811.11514, [[arXiv:astro-ph.GA/1811.11514](https://arxiv.org/abs/astro-ph.GA/1811.11514)].
 49. Sillanpää, A.; Teerikorpi, P.; Haarala, S.; Korhonen, T.; Efimov, I.S.; Shakhovskoi, N.M. Similar structures in the outbursts of OJ 287 in 1972 and 1983. *A&A* **1985**, *147*, 67–70.

50. Sillanpaa, A.; Takalo, L.O.; Pursimo, T.; Lehto, H.J.; Nilsson, K.; Teerikorpi, P.; Heinaemaeki, P.; Kidger, M.; de Diego, J.A.; Gonzalez-Perez, J.N.; Rodriguez-Espinosa, J.M.; Mahoney, T.; Boltwood, P.; Dultzin-Hacyan, D.; Benitez, E.; Turner, G.W.; Robertson, J.W.; Honeycut, R.K.; Efimov, Y.S.; Shakhovskoy, N.; Charles, P.A.; Schramm, K.J.; Borgeest, U.; Linde, J.V.; Weneit, W.; Kuehl, D.; Schramm, T.; Sadun, A.; Grashuis, R.; Heidt, J.; Wagner, S.; Bock, H.; Kuemmel, M.; Heines, A.; Fiorucci, M.; Tosti, G.; Ghisellini, G.; Raiteri, C.M.; Villata, M.; de Francesco, G.; Bosio, S.; Latini, G. Confirmation of the 12-year optical outburst cycle in blazar OJ 287. *A&A* **1996**, *305*, L17.
51. Sillanpaa, A.; Takalo, L.O.; Pursimo, T.; Nilsson, K.; Heinamaki, P.; Katajainen, S.; Pietila, H.; Hanski, M.; Rekola, R.; Kidger, M.; Boltwood, P.; Turner, G.W.; Robertson, J.W.; Honeycut, R.K.; Efimov, Y.S.; Shakhovskoy, N.; Fiorucci, M.; Tosti, G.; Ghisellini, G.; Raiteri, C.M.; Villata, M.; de Francesco, G.; Lanteri, L.; Chiaberge, M.; Peila, A.; Heidt, J. Double-peak structure in the cyclic optical outbursts of blazar OJ 287. *A&A* **1996**, *315*, L13–L16.
52. Sundelius, B.; Wahde, M.; Lehto, H.J.; Valtonen, M.J. A Numerical Simulation of the Brightness Variations of OJ 287. *ApJ* **1997**, *484*, 180–185. doi:10.1086/304331.
53. Tanaka, T.L. Recurring flares from supermassive black hole binaries: implications for tidal disruption candidates and OJ 287. *MNRAS* **2013**, *434*, 2275–2288, [1303.6279]. doi:10.1093/mnras/stt1164.
54. Villata, M.; Raiteri, C.M.; Sillanpaa, A.; Takalo, L.O. A beaming model for the OJ 287 periodic optical outbursts. *MNRAS* **1998**, *293*, L13–L16. doi:10.1046/j.1365-8711.1998.01244.x.
55. Valtaoja, E.; Teräsraanta, H.; Tornikoski, M.; Sillanpää, A.; Aller, M.F.; Aller, H.D.; Hughes, P.A. Radio Monitoring of OJ 287 and Binary Black Hole Models for Periodic Outbursts. *ApJ* **2000**, *531*, 744–755. doi:10.1086/308494.
56. Shi, W.; Liu, X.; Song, H. A new model for the periodic outbursts of the BL Lac object OJ287. *Ap&SS* **2007**, *310*, 59–63. doi:10.1007/s10509-007-9413-z.
57. Villforth, C.; Nilsson, K.; Heidt, J.; Takalo, L.O.; Pursimo, T.; Berdyugin, A.; Lindfors, E.; Pasanen, M.; Winiarski, M.; Drozd, M.; Ogloza, W.; Kurpinska-Winiarska, M.; Siwak, M.; Koziel-Wierzbowska, D.; Porowski, C.; Kuzmicz, A.; Krzesinski, J.; Kundera, T.; Wu, J.H.; Zhou, X.; Efimov, Y.; Sadakane, K.; Kamada, M.; Ohlert, J.; Hentunen, V.P.; Nissinen, M.; Dietrich, M.; Assef, R.J.; Atlee, D.W.; Bird, J.; Depoy, D.L.; Eastman, J.; Peebles, M.S.; Prieto, J.; Watson, L.; Yee, J.C.; Liakos, A.; Niarchos, P.; Gazeas, K.; Dogru, S.; Donmez, A.; Marchev, D.; Coggins-Hill, S.A.; Mattingly, A.; Keel, W.C.; Haque, S.; Aungwerojwit, A.; Bergvall, N. Variability and stability in blazar jets on time-scales of years: optical polarization monitoring of OJ 287 in 2005–2009. *MNRAS* **2010**, *402*, 2087–2111, [0912.0005]. doi:10.1111/j.1365-2966.2009.16133.x.
58. Qian, S.J. Model simulation for periodic double-peaked outbursts in blazar OJ 287: binary black hole plus lighthouse effect. *Research in Astronomy and Astrophysics* **2015**, *15*, 687. doi:10.1088/1674-4527/15/5/007.
59. Pursimo, T.; Takalo, L.O.; Sillanpää, A.; Kidger, M.; Lehto, H.J.; Heidt, J.; Charles, P.A.; Aller, H.; Aller, M.; Beckmann, V.; Benítez, E.; Bock, H.; Boltwood, P.; Borgeest, U.; de Diego, J.A.; De Francesco, G.; Dietrich, M.; Dultzin-Hacyan, D.; Efimov, Y.; Fiorucci, M.; Ghisellini, G.; González-Pérez, N.; Hanski, M.; Heinämäki, P.; Honeycutt, R.K.; Hughes, P.; Karlamaa, K.; Katajainen, S.; Knee, L.B.G.; Kurtanidze, O.M.; Kümmel, M.; Kühl, D.; Lainela, M.; Lanteri, L.; Linde, J.V.; Lähteenmäki, A.; Maesano, M.; Mahoney, T.; Marchenko, S.; Marscher, A.; Massaro, E.; Montagni, F.; Nesci, R.; Nikolashvili, M.; Nilsson, K.; Nurmi, P.; Pietilä, H.; Poyner, G.; Raiteri, C.M.; Rekola, R.; Richter, G.M.; Riehoainen, A.; Robertson, J.W.; Rodríguez-Espinoza, J.M.; Sadun, A.; Shakhovskoy, N.; Schramm, K.J.; Schramm, T.; Sobrito, G.; Teerikorpi, P.; Teräsraanta, H.; Tornikoski, M.; Tosti, G.; Turner, G.W.; Valtaoja, E.; Valtonen, M.; Villata, M.; Wagner, S.J.; Webb, J.; Weneit, W.; Wiren, S. Intensive monitoring of OJ 287. *A&AS* **2000**, *146*, 141–155. doi:10.1051/aas:2000264.
60. Kushwaha, P.; Gupta, A.C.; Wiita, P.J.; Gaur, H.; de Gouveia Dal Pino, E.M.; Bhagwan, J.; Kurtanidze, O.M.; Larionov, V.M.; Damjanovic, G.; Uemura, M.; Semkov, E.; Strigachev, A.; Bachev, R.; Vince, O.; Gu, M.; Zhang, Z.; Abe, T.; Agarwal, A.; Borman, G.A.; Fan, J.H.; Grishina, T.S.; Hirochi, J.; Itoh, R.; Kawabata, M.; Kopatskaya, E.N.; Kurtanidze, S.O.; Larionova, E.G.; Larionova, L.V.; Mishra, A.; Morozova, D.A.; Nakaoka, T.; Nikolashvili, M.G.; Savchenko, S.S.; Troitskaya, Y.V.; Troitsky, I.S.; Vasilyev, A.A. Multiwavelength temporal and spectral variability of the blazar OJ 287 during and after the 2015 December flare: a major accretion disc contribution. *MNRAS* **2018**, *473*, 1145–1156, [arXiv:astro-ph.HE/1709.04957]. doi:10.1093/mnras/stx2394.
61. Hudec, R.; Bašta, M.; Pihajoki, P.; Valtonen, M. The historical 1900 and 1913 outbursts of the binary blazar candidate OJ287. *A&A* **2013**, *559*, A20. doi:10.1051/0004-6361/201219323.

62. Valtonen, M.J.; Zola, S.; Ciprini, S.; Gopakumar, A.; Matsumoto, K.; Sadakane, K.; Kidger, M.; Gazeas, K.; Nilsson, K.; Berdyugin, A.; Pirola, V.; Jermak, H.; Baliyan, K.S.; Alicavus, F.; Boyd, D.; Campas Torrent, M.; Campos, F.; Carrillo Gómez, J.; Caton, D.B.; Chavushyan, V.; Dalessio, J.; Debski, B.; Dimitrov, D.; Drozd, M.; Er, H.; Erdem, A.; Escartin Pérez, A.; Fallah Ramazani, V.; Filippenko, A.V.; Ganesh, S.; Garcia, F.; Gómez Pinilla, F.; Gopinathan, M.; Haislip, J.B.; Hudec, R.; Hurst, G.; Ivarsen, K.M.; Jelinek, M.; Joshi, A.; Kagitani, M.; Kaur, N.; Keel, W.C.; LaCluyze, A.P.; Lee, B.C.; Lindfors, E.; Lozano de Haro, J.; Moore, J.P.; Mugrauer, M.; Naves Noguees, R.; Neely, A.W.; Nelson, R.H.; Ogloza, W.; Okano, S.; Pandey, J.C.; Perri, M.; Pihajoki, P.; Poyner, G.; Provencal, J.; Pursimo, T.; Raj, A.; Reichart, D.E.; Reinthal, R.; Sadegi, S.; Sakanoi, T.; Salto González, J.L.; Sameer.; Schweyer, T.; Siwak, M.; Soldán Alfaro, F.C.; Sonbas, E.; Steele, I.; Stocke, J.T.; Strobl, J.; Takalo, L.O.; Tomov, T.; Tremosa Espasa, L.; Valdes, J.R.; Valero Pérez, J.; Verrecchia, F.; Webb, J.R.; Yoneda, M.; Zejmo, M.; Zheng, W.; Telting, J.; Saario, J.; Reynolds, T.; Kvammen, A.; Gafton, E.; Karjalainen, R.; Harmanen, J.; Blay, P. Primary Black Hole Spin in OJ 287 as Determined by the General Relativity Centenary Flare. *ApJL* **2016**, *819*, L37. doi:10.3847/2041-8205/819/2/L37.
63. Siejkowski, H.; Wierzcholska, A. Characterizing long-term optical, ultraviolet and X-ray variability in different activity states of OJ 287. *MNRAS* **2017**, *468*, 426–434. doi:10.1093/mnras/stx495.
64. Kapanadze, B.; Vercellone, S.; Romano, P.; Hughes, P.; Aller, M.; Aller, H.; Kapanadze, S.; Tabagari, L. Strong X-ray flaring activity of the BL Lacertae source OJ 287 in 2016 October–2017 April. *MNRAS* **2018**, *480*, 407–430. doi:10.1093/mnras/sty1803.
65. Agudo, I.; Marscher, A.P.; Jorstad, S.G.; Gómez, J.L.; Perucho, M.; Piner, B.G.; Rioja, M.; Dodson, R. Erratic Jet Wobbling in the BL Lacertae Object OJ287 Revealed by Sixteen Years of 7 mm VLBA Observations. *ApJ* **2012**, *747*, 63. [arXiv:astro-ph.CO/1112.4747]. doi:10.1088/0004-637X/747/1/63.
66. Gupta, A.C.; Gaur, H.; Wiita, P.J.; Pandey, A.; Kushwaha, P.; Hu, S.M.; Kurtanidze, O.M.; Semkov, E.; Damjanovic, G.; Goyal, A.; Uemura, M.; Darriba, A.; Chen, X.; Vince, O.; Gu, M.F.; Zhang, Z.; Bachev, R.; Chanishvili, R.; Itoh, R.; Kawabata, M.; Kurtanidze, S.O.; Nakaoka, T.; Nikolashvili, M.G.; Stawarz, L.; Strigachev, A. Characterizing Optical Variability of OJ 287 in 2016–2017. *AJ* **2019**, *157*, 95. [arXiv:astro-ph.HE/1803.03964]. doi:10.3847/1538-3881/aaf7d.
67. Cohen, M.H.; Aller, H.D.; Aller, M.F.; Hovatta, T.; Kharb, P.; Kovalev, Y.Y.; Lister, M.L.; Meier, D.L.; Pushkarev, A.B.; Savolainen, T. Reversals in the Direction of Polarization Rotation in OJ 287. *ApJ* **2018**, *862*, 1. doi:10.3847/1538-4357/aac31.
68. D’arcangelo, F.D.; Marscher, A.P.; Jorstad, S.G.; Smith, P.S.; Larionov, V.M.; Hagen-Thorn, V.A.; Williams, G.G.; Gear, W.K.; Clemens, D.P.; Sarcia, D.; Grabau, A.; Tollestrup, E.V.; Buie, M.W.; Taylor, B.; Dunham, E. Synchronous Optical and Radio Polarization Variability in the Blazar OJ287. *ApJ* **2009**, *697*, 985–995. [arXiv:astro-ph.CO/0903.3934]. doi:10.1088/0004-637X/697/2/985.
69. O’Brien, S. VERITAS detection of VHE emission from the optically bright quasar OJ 287. *ArXiv e-prints* **2017**, p. arXiv:1708.02160. [arXiv:astro-ph.HE/1708.02160].
70. Worrall, D.M.; Puschell, J.J.; Jones, B.; Bruhweiler, F.C.; Aller, M.F.; Aller, H.D.; Hodge, P.E.; Sitko, M.L.; Stein, W.A.; Zhang, Y.X.; Ku, W.H.M. Two multifrequency observations of the BL Lacertae object OJ 287. *ApJ* **1982**, *261*, 403–411. doi:10.1086/160352.
71. Gear, W.K.; Robson, E.I.; Brown, L.M.J. Infrared variability of the BL Lacertae object OJ287 since its outburst in 1983. *Nature* **1986**, *324*, 546. doi:10.1038/324546a0.
72. Hagen-Thorn, V.A.; Marchenko, S.G.; Takalo, L.O.; Sillanpää, A.; Pursimo, T.; Boltwood, P.; Kidger, M.; Gonzalez-Perez, J.N. The variable sources responsible for the photometric behaviour of OJ 287 in the IR-optical-UV region during 1993–1996. *AA&S* **1998**, *133*, 353–359. doi:10.1051/aas:1998326.
73. Idesawa, E.; Tashiro, M.; Makishima, K.; Kubo, H.; Otani, C.; Fujimoto, R.; Kii, T.; Makino, F.; Takahashi, T.; Ueda, Y.; Ohashi, T. X-Ray Observations of the BL Lacertae Object OJ 287 with ASCA. *PASJ* **1997**, *49*, 631–637. doi:10.1093/pasj/49.6.631.
74. Isobe, N.; Tashiro, M.; Sugiho, M.; Makishima, K. ASCA Observations of the BL Lacertae Object OJ 287 in 1997 April and November. *PASJ* **2001**, *53*, 79–84. [astro-ph/0011046]. doi:10.1093/pasj/53.1.79.
75. Shrader, C.R.; Hartman, R.C.; Webb, J.R. Probable detection of high-energy gamma-ray emission from OJ 287 during a major optical flare. *A&AS* **1996**, *120*, 599–602.
76. Pal, M.; Kushwaha, P.; Dewangan, G.C.; Sami, M.; Pawar, P.K. Strong Soft X-ray Excess in 2015 XMM-Newton Observation of BL–Lac OJ~287. *arXiv e-prints* **2019**, p. arXiv:1912.02730. [arXiv:astro-ph.HE/1912.02730].

77. Dey, L.; Valtonen, M.J.; Gopakumar, A.; Zola, S.; Hudec, R.; Pihajoki, P.; Ciprini, S.; Matsumoto, K.; Sadakane, K.; Kidger, M.; Nilsson, K.; Mikkola, S.; Sillanpää, A.; Takalo, L.O.; Lehto, H.J.; Berdyugin, A.; Pirola, V.; Jermak, H.; Baliyan, K.S.; Pursimo, T.; Caton, D.B.; Alicavus, F.; Baransky, A.; Blay, P.; Boumis, P.; Boyd, D.; Campas Torrent, M.; Campos, F.; Carrillo Gómez, J.; Chandra, S.; Chavushyan, V.; Dalessio, J.; Debski, B.; Drozd, M.; Er, H.; Erdem, A.; Escartin Pérez, A.; Fallah Ramazani, V.; Filippenko, A.V.; Gafton, E.; Ganesh, S.; Garcia, F.; Gazeas, K.; Godunova, V.; Gómez Pinilla, F.; Gopinathan, M.; Haislip, J.B.; Harmanen, J.; Hurst, G.; Janík, J.; Jelinek, M.; Joshi, A.; Kagitani, M.; Karjalainen, R.; Kaur, N.; Keel, W.C.; Kouprianov, V.V.; Kundera, T.; Kurowski, S.; Kvammen, A.; LaCluyze, A.P.; Lee, B.C.; Liakos, A.; Lindfors, E.; Lozano de Haro, J.; Mugrauer, M.; Naves Nogue, R.; Neely, A.W.; Nelson, R.H.; Ogloza, W.; Okano, S.; Pajdosz-Śmierciak, U.; Pandey, J.C.; Perri, M.; Poyner, G.; Provencal, J.; Raj, A.; Reichart, D.E.; Reinthal, R.; Reynolds, T.; Saario, J.; Sadegi, S.; Sakanoi, T.; Salto González, J.L.; Sameer.; Schweyer, T.; Simon, A.; Siwak, M.; Soldán Alfaro, F.C.; Sonbas, E.; Steele, I.; Stocke, J.T.; Strobl, J.; Tomov, T.; Tremosa Espasa, L.; Valdes, J.R.; Valero Pérez, J.; Verrecchia, F.; Vasylenko, V.; Webb, J.R.; Yoneda, M.; Zejmo, M.; Zheng, W.; Zielinski, P. Authenticating the Presence of a Relativistic Massive Black Hole Binary in OJ 287 Using Its General Relativity Centenary Flare: Improved Orbital Parameters. *ApJ* **2018**, *866*, 11, [[arXiv:astro-ph.HE/1808.09309](https://arxiv.org/abs/1808.09309)]. doi:10.3847/1538-4357/aadd95.
78. Gupta, A.C.; Agarwal, A.; Mishra, A.; Gaur, H.; Wiita, P.J.; Gu, M.F.; Kurtanidze, O.M.; Damljanovic, G.; Uemura, M.; Semkov, E.; Strigachev, A.; Bachev, R.; Vince, O.; Zhang, Z.; Villarroel, B.; Kushwaha, P.; Pandey, A.; Abe, T.; Chanishvili, R.; Chigladze, R.A.; Fan, J.H.; Hirochi, J.; Itoh, R.; Kanda, Y.; Kawabata, M.; Kimeridze, G.N.; Kurtanidze, S.O.; Latev, G.; Dimitrova, R.V.M.; Nakaoka, T.; Nikolashvili, M.G.; Shiki, K.; Sigua, L.A.; Spassov, B. Multiband optical variability of the blazar OJ 287 during its outbursts in 2015-2016. *MNRAS* **2017**, *465*, 4423–4433, [[arXiv:astro-ph.HE/1611.07561](https://arxiv.org/abs/1611.07561)]. doi:10.1093/mnras/stw3045.
79. Frohlich, A.; Goldsmith, S.; Weistrop, D. Further studies of the optical variability of OJ 287. *MNRAS* **1974**, *168*, 417–426. doi:10.1093/mnras/168.2.417.
80. Pihajoki, P.; Valtonen, M.; Ciprini, S. Short time-scale periodicity in OJ 287. *MNRAS* **2013**, *434*, 3122–3129, [[arXiv:astro-ph.HE/1307.1113](https://arxiv.org/abs/1307.1113)]. doi:10.1093/mnras/stt1233.
81. Bhatta, G.; Zola, S.; Stawarz, L.; Ostrowski, M.; Winiarski, M.; Ogloza, W.; Drózd, M.; Siwak, M.; Liakos, A.; Kozieł-Wierzbowska, D.; Gazeas, K.; Debski, B.; Kundera, T.; Stachowski, G.; Paliya, V.S. Detection of Possible Quasi-periodic Oscillations in the Long-term Optical Light Curve of the BL Lac Object OJ 287. *ApJ* **2016**, *832*, 47, [[arXiv:astro-ph.HE/1609.02388](https://arxiv.org/abs/1609.02388)]. doi:10.3847/0004-637X/832/1/47.
82. Valtaoja, E.; Lehto, H.; Teerikorpi, P.; Korhonen, T.; Valtonen, M.; Teräsranta, H.; Salonen, E.; Urpo, S.; Tiuri, M.; Pirola, V.; Saslaw, W.C. A 15.7-min periodicity in OJ287. *Nature* **1985**, *314*, 148–149. doi:10.1038/314148a0.
83. Roberts, D.H.; Gabuzda, D.C.; Wardle, J.F.C. Linear polarization structure of the BL Lacertae object OJ 287 at milliarcsecond resolution. *ApJ* **1987**, *323*, 536–542. doi:10.1086/165849.
84. Tateyama, C.E.; Kingham, K.A. Structure of OJ 287 from Geodetic VLBA Data. *ApJ* **2004**, *608*, 149–156. doi:10.1086/392524.
85. Cohen, M. OJ 287 as a Rotating Helix. *Galaxies* **2017**, *5*, 12. doi:10.3390/galaxies5010012.
86. Agudo, I.; Jorstad, S.G.; Marscher, A.P.; Larionov, V.M.; Gómez, J.L.; Lähteenmäki, A.; Gurwell, M.; Smith, P.S.; Wiesemeyer, H.; Thum, C.; Heidt, J.; Blinov, D.A.; D’Arcangelo, F.D.; Hagen-Thorn, V.A.; Morozova, D.A.; Nieppola, E.; Roca-Sogorb, M.; Schmidt, G.D.; Taylor, B.; Tornikoski, M.; Troitsky, I.S. Location of γ -ray Flare Emission in the Jet of the BL Lacertae Object OJ287 More than 14 pc from the Central Engine. *ApJL* **2011**, *726*, L13, [[1011.6454](https://arxiv.org/abs/1011.6454)]. doi:10.1088/2041-8205/726/1/L13.
87. Hodgson, J.A.; Krichbaum, T.P.; Marscher, A.P.; Jorstad, S.G.; Rani, B.; Marti-Vidal, I.; Bach, U.; Sanchez, S.; Bremer, M.; Lindqvist, M.; Uunila, M.; Kallunki, J.; Vicente, P.; Fuhrmann, L.; Angelakis, E.; Karamanavis, V.; Myserlis, I.; Nestoras, I.; Chidiac, C.; Sievers, A.; Gurwell, M.; Zensus, J.A. Location of γ -ray emission and magnetic field strengths in OJ 287. *A&A* **2017**, *597*, A80, [[arXiv:astro-ph.HE/1607.00725](https://arxiv.org/abs/1607.00725)]. doi:10.1051/0004-6361/201526727.
88. Wright, S.C.; McHardy, I.M.; Abraham, R.G. Host galaxies of the optically violently variable quasars PKS 0736+017, OJ 287 and LB 2136. *MNRAS* **1998**, *295*, 799–812. doi:10.1046/j.1365-8711.1998.01248.x.
89. Heidt, J.; Nilsson, K.; Appenzeller, I.; Jäger, K.; Seifert, W.; Szeifert, T.; Gässler, W.; Häfner, R.; Hummel, W.; Muschielok, B.; Nicklas, H.; Stahl, O. Observations of the host galaxies of the BL Lacertae objects H 0414+009 and OJ 287 with FORS1 at VLT-UT1. *A&A* **1999**, *352*, L11–L16.

90. Valtonen, M.J.; Dey, L.; Hudec, R.; Zola, S.; Gopakumar, A.; Mikkola, S.; Ciprini, S.; Matsumoto, K.; Sadakane, K.; Kidger, M.; Gazeas, K.; Nilsson, K.; Berdyugin, A.; Piirola, V.; Jermak, H.; Baliyan, K.S.; Reichart, D.E.; Haque, S.; the OJ287-15/16 Collaboration. High accuracy measurement of gravitational wave back-reaction in the OJ287 black hole binary. *ArXiv e-prints* **2018**, p. arXiv:1810.00566, [[arXiv:astro-ph.HE/1810.00566](https://arxiv.org/abs/1810.00566)].
91. Takalo, L.O.; Kidger, M.; de Diego, J.A.; Sillanpää, A.; Piirola, V.; Terasranta, H. A sudden fade of OJ 287. *A&AS* **1990**, *83*, 459–465.
92. Sasada, M.; Jorstad, S.; Marscher, A.P.; Bala, V.; Joshi, M.; MacDonald, N.R.; Malmrose, M.P.; Larionov, V.M.; Morozova, D.A.; Troitsky, I.S.; Agudo, I.; Casadio, C.; Gómez, J.L.; Molina, S.N.; Itoh, R. Optical Emission and Particle Acceleration in a Quasi-stationary Component in the Jet of OJ 287. *ApJ* **2018**, *864*, 67, [[arXiv:astro-ph.HE/1807.11145](https://arxiv.org/abs/1807.11145)]. doi:10.3847/1538-4357/aad553.
93. Kikuchi, S.; Inoue, M.; Mikami, Y.; Tabara, H.; Kato, T. A synchronous variation of polarization angle in OJ 287 in the optical and radio regions. *A&A* **1988**, *190*, L8–L10.
94. Madejski, G.; Sikora, M. Gamma-Ray Observations of Active Galactic Nuclei. *ARAA* **2016**, *54*, 725–760. doi:10.1146/annurev-astro-081913-040044.
95. Pihajoki, P. Black hole accretion disc impacts. *MNRAS* **2016**, *457*, 1145–1161, [[arXiv:astro-ph.HE/1510.07642](https://arxiv.org/abs/1510.07642)]. doi:10.1093/mnras/stv3023.
96. Valtonen, M.J.; Ciprini, S.; Lehto, H.J. On the masses of OJ287 black holes. *MNRAS* **2012**, *427*, 77–83, [[arXiv:astro-ph.HE/1208.0906](https://arxiv.org/abs/1208.0906)]. doi:10.1111/j.1365-2966.2012.21861.x.
97. Valtonen, M.J.; Mikkola, S.; Merritt, D.; Gopakumar, A.; Lehto, H.J.; Hyvönen, T.; Rampadarath, H.; Saunders, R.; Basta, M.; Hudec, R. Measuring the Spin of the Primary Black Hole in OJ287. *ApJ* **2010**, *709*, 725–732, [[arXiv:astro-ph.HE/0912.1209](https://arxiv.org/abs/0912.1209)]. doi:10.1088/0004-637X/709/2/725.
98. Qian, S. Model simulation of optical light curves for blazar OJ287. *arXiv e-prints* **2019**, p. arXiv:1904.03357, [[arXiv:astro-ph.GA/1904.03357](https://arxiv.org/abs/1904.03357)].
99. Oikonomou, F.; Murase, K.; Padovani, P.; Resconi, E.; Meszaros, P. High-energy neutrinos from individual blazar flares. 36th International Cosmic Ray Conference (ICRC2019), 2019, Vol. 36, *International Cosmic Ray Conference*, p. 971, [[arXiv:astro-ph.HE/1906.05302](https://arxiv.org/abs/1906.05302)].
100. Kushwaha, P.; de Gouveia Dal Pino, E.M.; Gupta, A.C.; Wiita, P.J. Revealing the Nature and Location of High Energy Emission in the Candidate Binary SMBH System OJ 287. PoS(BHCB2018), 2019, Vol. 329, *Proceeding of Science*, p. 22, [[arXiv:astro-ph.HE/1901.10768](https://arxiv.org/abs/1901.10768)]. doi:10.22323/1.329.0022.
101. Valtonen, M.J.; Zola, S.; Pihajoki, P.; Enestam, S.; Lehto, H.J.; Dey, L.; Gopakumar, A.; Drozd, M.; Ogłóza, W.; Zejmo, M.; Gupta, A.C.; Pursimo, T.; Ciprini, S.; Kidger, M.; Nilsson, K.; Berdyugin, A.; Piirola, V.; Jermak, H.; Hudec, R.; Laine, S. Accretion Disk Parameters Determined from the Great 2015 Flare of OJ 287. *ApJ* **2019**, *882*, 88, [[arXiv:astro-ph.HE/1907.11011](https://arxiv.org/abs/1907.11011)]. doi:10.3847/1538-4357/ab3573.
102. Nilsson, K.; Takalo, L.O.; Lehto, H.J.; Sillanpää, A. H-alpha monitoring of OJ 287 in 2005-08. *A&A* **2010**, *516*, A60, [[arXiv:astro-ph.CO/1004.2617](https://arxiv.org/abs/1004.2617)]. doi:10.1051/0004-6361/201014198.